AD-A092 629 UNIVERSITY COLL LONDON (ENGLAND) DEPT OF PHYSICS AND--ETC F/G 4/1
OZONE AND WIND VARIATIONS IN THE STRATOSPHERE AND MESOSPHERE.(U)
DEC 78 G V GROVES, R J LUCAS AFOSR-77-3224

UNCLASSIFIED AFGL-TR-80-0349 NL

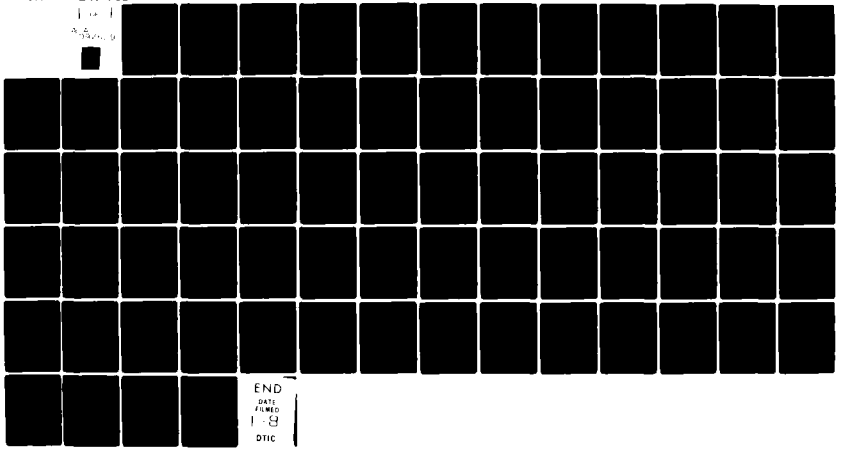

END
DATE FILMED
1-81
DTIC

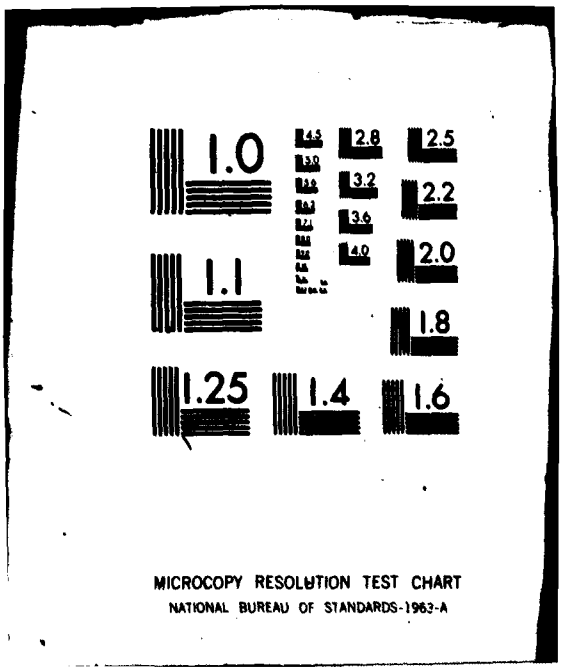
1.0
1.1
1.25
1.4
1.6
1.8
2.0
2.2
2.5
2.8
3.2
3.6
4.0
MICROCOPY RESOLUTION TEST CHART
NATIONAL BUREAU OF STANDARDS-1963-A

Grant number: AFOSR-77-3224

OZONE AND WIND VARIATIONS IN THE STRATOSPHERE AND MESOSPHERE

G. V. Groves and R. J. Lucas
Department of Physics and Astronomy,
University College London,
Gower Street, London WC1E 6BT,
England.

31 December 1978

Scientific Report No. 2

1 December 1976 - 31 October 1978

Approved for public release; distribution unlimited.

Prepared for:

Air Force Geophysics Laboratory,
L. G. Hanscom Field, Bedford, Massachusetts 01730, USA.

and

European Office of Aerospace Research and Development,
London, England.

REPORT DOCUMENTATION PAGE	READ INSTRUCTIONS BEFORE COMPLETING FORM
1. Report Number: AFGL-TR-80-0349	2. Govt Accession No.: AD-A092 629	3. Recipient's Catalog Number
4. Title (and Subtitle): OZONE AND WIND VARIATIONS IN THE STRATOSPHERE AND MESOSPHERE.	5. Type of Report & Period Covered: Scientific Report No. 2, 76 Dec 01 - 78 Oct 31
	6. Performing Org. Report Number
7. Author(s): GERALD V. GROVES and ROBERT J. LUCAS	8. Contract or Grant Number: AFOSR-77-3224
9. Performing Organization Name and Address: Department of Physics and Astronomy, University College London, Gower Street, London WC1E 6BT, ENGLAND.	10. Program Element, Project, Task Area & Work Unit Numbers: 62101F, 668705AJ
11. Controlling Office Name and Address: Air Force Geophysics Laboratory/LKD, Hanscom AFB, MA 01731, Monitor/William K. Vickery/LKD	12. Report Date: 78 Dec 31
	13. Number of Pages: 71
14. Monitoring Agency Name and Address: European Office of Aerospace Research and Development/LNG, Box 14, FPO New York 09510	15.
16. & 17. Distribution Statement: Approved for public release; distribution unlimited.	
18. Supplementary Notes	
19. Key Words: OZONE, WINDS, STRATOSPHERE, MESOSPHERE, MIDDLE ATMOSPHERE, SEASONAL, DIURNAL	

20. Abstract

1. A latitudinal and seasonal model for ozone concentrations to 75 km is presented. At the lower altitudes the model is based on Umkehr data from the world ozone network and at the higher altitudes on rocket and satellite data as well as some ground-based measurements. The model is tabulated for the four seasons and latitudes 0° to 60°N in steps of 15° for each 5 km height interval from 10 to 75 km.

2. Seasonal wind variations in the mesosphere are reviewed and a mean meridional circulation is inferred for the winter hemisphere.

3. Diurnal and semidiurnal wind oscillations at heights between 25 and 60 km are presented being the results of a comprehensive analysis of data from short series of rocket launchings held at various western hemisphere sites between 1965 and 1974.

FORM 1473

361070

A latitudinal and seasonal ozone model to 75 km

R. J. Lucas

Department of Physics and Astronomy,

University College London,

England

Abstract

An ozone model based on Umkehr data from the world ozone network at the lower altitudes and on the available rocket and satellite data at the higher altitudes as well as ground-based techniques is presented. The model is tabulated for the four seasons and latitudes 0° to 60°N in steps of 15° for each 5 km height interval from 10 to 75 km. The model is compared with current photochemistry results with which a significant disagreement is found at the solstices. Above 50 km a model for the relative daytime ozone variation based on the photochemistry of Parks and London (1974) is presented.

CONTENTS

1. The need for an ozone model

An ozone model was required to enable the Hough modes of the heating rate in the stratosphere to be calculated. Ideally a model giving values for each height, latitude and longitude was desired, but as a first approximation the longitudinal variation was ignored, being significant only below about 35 km where ozone lifetimes are sufficiently long for transport mechanisms to be important: this approximation is discussed in Section 4(ii). It was decided to further restrict the model to latitudes of less than 60° as data at higher latitudes is scarce: for evaluating positive Hough modes this representation is adequate as these modes rapidly approach zero at higher latitudes. It is necessary to have an accurate ozone height profile in order to obtain the corresponding heating profile and to derive from this the positive mode contributions. Most of the ozone heating occurs between 20 and 60 km: by 80 km there is very little heating and above the mesopause absorption by molecular and atomic oxygen become the dominant heat sources: therefore a height range of 10-75 km was taken. As the heating rate would need to be calculated for any time of the year, four seasonal models were a minimum requirement. Seasonal symmetry has been assumed between the N and S hemispheres, i.e. January in the N hemisphere corresponds to July in the S hemisphere and similarly for April and October. This is justified as the higher latitudes where there is a marked asymmetry are excluded: see Kulkarni (1962) and also the discussion below (Section 4).

The only existing model known to us that suited this specification was by Parks and London (1974): this was based for the 15-50 km region on observational data and for the 50-80 km region on photochemical theory. We required our model to rely more heavily on observational results especially the more recent data from rocket flown sondes and satellites: the photochemical model was retained for comparison.

2. The data

For the lower altitudes Umkehr data were primarily used; other data being plotted mainly for comparison and also to help at latitudes poorly covered by the Umkehr stations. Data were taken from the summaries for all years for each station included in the years 1973-76 of 'Ozone data for the world'. The good world wide distribution of stations using the Umkehr technique and the length of time that some of the data have been collected make this method ideal for a synoptic survey, whilst the main disadvantage of the Umkehr method, the lack of fine detail in vertical structure, is not important as this would tend to be averaged out over several observations.

Between 40 and 60 km a large part of the data came from Krueger et al. (1973) which describes the results from the Nimbus satellite, and from London and Frederick (1977) which gives the Ogo satellite results: these data have the advantage of being well distributed latitudinally and being in most cases derived from several observations.

Above 55 km the available data become extremely tenuous, with no consistent series of observations from more than one latitude. The situation is made more acute by the restriction to daytime values as at altitudes in excess of 50 km there is a significant diurnal ozone variation. The variety of techniques used at the higher altitudes might to some extent explain the large dispersion evident at these heights. The Nimbus and Ogo satellites used backscatter ultra-violet instruments, some of the rocket soundings used optical spectrographs to measure direct attenuation of ultra-violet light as well as electrochemical sondes and chemiluminescent detectors. The key to the diagrams indicates the technique used for each source of data.

3. The method

A height interval of 5 km was chosen at which to plot the number density for latitudes 60°N to 60°S. This provides the same order of resolution as the Umkehr data, where nine layers cover 5 to 45 km. The values at the 5 km intervals were interpolated from the values at the Umkehr levels.

The model is devised for January, July, April and October, and for altitudes below 50 km, where there is no lack of good observations, only results from these months were used. At higher altitudes, where data become increasingly scarce, data from dates up to a month either side of the above months were included.

Where it was possible to plot error bars this was done: for the Umkehr results these were ± one standard deviation divided by the root of the number of observations (the standard error of the mean). This value was used whenever it could be calculated or was given, otherwise an estimate was made from examining techniques used in the measurement and any other relevant factors. This was essential as it was necessary to be able to weight points according to their accuracy when there were few plotted values to enable a meaningful best fit to be drawn. For the determination of the best fit lines giving the latitude dependence of the number density, there are three altitude regions that were dealt with differently.

(i) 10-35 km. Figs. 1-6, and 15-20.

The latitudinal dependence is well defined by the Umkehr data enabling a smooth line to be drawn by eye: this was preferable to doing a least squares fit as it was possible to gain some feel for where the line should go by examining the plots above and below the one in question and by taking into account the total ozone implied and comparing this with existing total

ozone models,(the total ozone is nearly completely specified by this region).

(ii) 40-45 km. Figs. 7,8,21 and 22.

Here the Umkehr data are less reliable as indicated by the relatively large error bars and a greater spread of the results making the Ogo and Nimbus satellite data extremely useful at these heights. The shape of the latitudinal dependence given by the Ogo data was consistent with that found by the Umkehr method at the lower level of 30 km, but was for both January/July and April/October about 15% higher, so in drawing the best fit at the 40 and 45 km levels the shapes of the Ogo results were retained and drawn at slightly higher values than indicated by the Umkehr results. The Ogo dataare given as being accurate to ± 10% and the resulting lines differ from the Ogo results by amounts between 0 and 40%. The Ogo results are plotted for these altitudes without error bars but simply as a dotted line: this was done to emphasise their shape.

(iii) 50-75 km. Figs. 9-14 and 23-28.

The points on these plots were weighted according to the size of their error bars and polynomial curves of up to order five were least squares fitted to them. The lowest order polynomial that gave a satisfactory fit was taken in all cases, for many of the plots the lack of data meant that this was a straight line. The January/July plots suffered from a bad latitude distribution of data, most points being clustered around ± 30° latitude.

When all the best fit lines had been established the results were tabulated and then smoothed vertically with a local smoothing formula, which used a least squares fit to five adjacent points to smooth the centre point. The smoothing was applied twice to log10 of the number density for the altitudes 35-75 km, the lower altitudes being omitted to avoid

diminishing the value at the ozone density maximum which occurs between 20 and 30 km. The smoothing made very little difference at most altitudes whilst removing the smaller scale irregularities: this helps if the model is to be used where any function of the ozone amount is differentiated with respect to height. The values after smoothing were plotted back onto the graphs as a check that they had not been altered to positions inconsistent with the data. These are the curves that are given in Figs. 1 to 28 and correspond to the values given in table 1.

4. Discussion on the resulting model

(i) 10-45 km

As the model presented here is based largely on Umkehr measurements it is to be expected that it will bear a close resemblence to previous models, notably Dütsch (1964). For the most part the latitude dependence is very similar. The very high values occurring on the April diagrams at 42°N come from station Goose, U.S.A.: Dütsch has marked on his plots a North American station at approximately this latitude that is consistently too high. If the Goose station values were correct the effect on the total ozone would be appreciable and inconsistent with existing total ozone models. Fig. 29 shows the seasonal,latitude dependence for the total ozone as calculated from the results given here. This compares well with London (1962) with slight differences of a few percent in actual values but with identical trends. The total ozone compares less well with that of Khrugian (1975) which shows the January and April values rather closer at latitudes higher than 30°.

As noted earlier the scatter at 40 km is significantly greater than at lower altitudes: this is not indicated on Dütsch's plots where he finds a greater scatter at the lowest heights due to daily changes

in the weather which show up because of the low number of readings taken by most of the stations. The model given here is less likely to suffer from this as a further ten years of data havebeen analysed. The greater scatter is probably due to an increase in the uncertainty of calculating the ozone amount at the uppermost levels inherent in the Umkehr method as is indicated by Dütsch et al. (1969) where two spectrophotometers were used simultaneously and the results compared. The profiles agreed extremely well at the lower levels and less well at the upper levels where the results became extremely sensitive to calibration errors. Also Dütsch and Ling (1969) compared Umkehr observations with those of an electrochemical sonde and found that, for the monthly means, the lowest and the two highest levels correlated the least well.

At 35 and 40 km the results are as much dependent on the satellite data as the Umkehr observations. The Ogo data of London and Frederick (1977) also shows that the assumption of seasonal symmetry between the two hemispheres may not be as good as has been previously supposed, with slightly higher mid-latitude southern hemisphere spring values than in the northern hemisphere. Dütsch commented on the asymmetry of the hemispheres in Dütsch (1974): by comparing results from Aspendale (38°S), Boulder (40°N), and New Mexico (35°N), he concluded that the largest differences were at the 10 mb level, which is too low to be substantiated by the Ogo data: however the differences were mostly less than 10%, and Dütsch pointed out that these were hardly significant considering the uncertainty of the soundings.

(ii) Longitudinal dependence

The model presented here takes no account of any longitudinal variations. A height dependent longitudinal model for 30-35 km can be obtained from London and Frederick (1977) which was derived from the Ogo satellite results. There are also several longitudinal total ozone models available. London and Frederick (1977) showed a maximum longitudinal variation at 35 km

of about 12% and detected very small variations as high as 50 km (0.7 mb) where it might be expected that the short ozone lifetimes would make geographical changes impossible to detect. The Nimbus satellite results of Krueger et al.(1973) found longitudinal variations up to the 4 mb level, but there is not sufficient data to enable a longitudinal model for all altitudes, say below 50 km, to be made. Manabe and Möller (1961) overcame this limitation by using the results of Tønsberg and Olsen (1943) which showed a one-to-one relationship between the total ozone and the vertical profile - if valid this result makes the vertical distributions given here redundant. Fig. 30 shows the vertical profiles taken from this report for April 30°N and October 45°N, that have very nearly the same total ozone but quite different profiles indicating that the approximation of Manabe and Möller (1961) is a poor one where detail in the vertical structure is important.

Until there are more surveys similar to the London and Frederick (1977) one, with information for a greater height range, it seems unlikely that a longitudinal model can be produced that successfully retains what is currently known about the ozone distribution.

(iii) 50-75 km

From the diagrams the most striking feature is the scarcity of available data for the altitudes above 60 km. Therefore it is stressed that the latitudinal dependences at these heights that have been deduced from this data are very uncertain.

As a comparison the photochemical model of Parks and London (1974) has been plotted on each of the diagrams, the April/October values for the photochemical model being the average of January and July values. At 50 km the latitude dependence for all the seasons is small and for January/July the latitude variation runs contrary to the photochemical model with

higher values in the winter, for any given latitude, than the summer. This is a continuation of the same trend as at 45 km where the Ogo and Nimbus satellite results and the Umkehr measurements show the same type of variation with latitude. At 50 km the main evidence for this trend was provided by the Ogo results and Watanabe and Tohmatsu (1976). The Ogo results stop at 55 km and the Watanabe and Tohmatsu(1976) continue up to 75 km, showing the same seasonal trend at each altitude. Their results are well documented with standard deviations and number of observations tabulated and provide the best available measurements at the highest altitudes. This same seasonal variation is also shown by Nagata et al. (1970) and for some of the heights by Johnson(1954). Evans and Llewellyn (1972) showed higher values for $O_2(^1\Delta g)$ emission for 60-65 km and over 80 km for June 1969 compared with December 1968: in equilibrium the emission rate has a simple relationship to the ozone amount, the emission being caused by photodissociation of ozone; and it is assumed that this is the only source of the emission. In Evans and Llewellyn (1969) the ozone densities have been calculated from the emission rates and these have been plotted. In general they are not in good agreement with other observations which may be due to the transition rate used in the conversion not being well enough determined. If this can be overcome this method of measuring ozone will be extremely useful not being restricted to taking measurements at dawn or dusk as some of the techniques are.

Watanabe and Tohmatsu (1976) explain the greater mesospheric winter ozone densities by suggesting there is an increase in the sinks for odd oxygen caused by an increase in the water vapour content of the atmosphere during the summer, water vapour providing the compounds H, OH and HO_2 which can then react with ozone. In the photochemical model of Parks and London (1974) the quantity of water vapour is assumed to be constant for all seasons and latitudes at each height. This is a reasonable approximation

higher values in the winter, for any given latitude, than the summer. This is a continuation of the same trend as at 45 km where the Ogo and Nimbus satellite results and the Umkehr measurements show the same type of variation with latitude. At 50 km the main evidence for this trend was provided by the Ogo results and Watanabe and Tohmatsu (1976). The Ogo results stop at 55 km and the Watanabe and Tohmatsu(1976) continue up to 75 km, showing the same seasonal trend at each altitude. Their results are well documented with standard deviations and number of observations tabulated and provide the best available measurements at the highest altitudes. This same seasonal variation is also shown by Nagata et al. (1970) and for some of the heights by Johnson(1954). Evans and Llewellyn (1972) showed higher values for $O_2(^1\Delta g)$ emission for 60-65 km and over 80 km for June 1969 compared with December 1968: in equilibrium the emission rate has a simple relationship to the ozone amount, the emission being caused by photodissociation of ozone; and it is assumed that this is the only source of the emission. In Evans and Llewellyn (1969) the ozone densities have been calculated from the emission rates and these have been plotted. In general they are not in good agreement with other observations which may be due to the transition rate used in the conversion not being well enough determined. If this can be overcome this method of measuring ozone will be extremely useful not being restricted to taking measurements at dawn or dusk as some of the techniques are.

Watanabe and Tohmatsu (1976) explain the greater mesospheric winter ozone densities by suggesting there is an increase in the sinks for odd oxygen caused by an increase in the water vapour content of the atmosphere during the summer, water vapour providing the compounds H, OH and HO_2 which can then react with ozone. In the photochemical model of Parks and London (1974) the quantity of water vapour is assumed to be constant for all seasons and latitudes at each height. This is a reasonable approximation

derived for 30°N in July, but by parameterising the daytime into equal divisions between sunrise and sunset the results have been extended for use at any latitude or time of year. The diurnal model assumes that the values for the ozone density are midday values. This may not be a good approximation as many of the measuring techniques are used near dawn or dusk so that the sunlight travels obliquely through the earth's atmosphere and there is sufficient attenuation for a measurement to be made. Photochemistry shows that it is at sunrise and sunset that the greatest variations in ozone density occur. During the night there are no sources of ozone and at dawn, the sudden 'switching on' of ultraviolet light rapidly dissociates the existing ozone. The ozone density gradually recovers during the day as atomic oxygen becomes available. At sunset, the major sink of ozone, photodissociation by the sun, is 'switched off' and production of ozone continues until the supply of atomic oxygen is depleted, hence the ozone density increases very rapidly. The Parks and London model, which was used to obtain the values in table 2, indicates an increase of approximately X 1.25 at 65 km, and X 2.5 at 70 km, at nightfall. These values are not well substantiated by some observations; Carver et al.(1972) suggested anything up to a tenfold increase between 60 and 70 km. Reigler et al. (1976) also show nighttime densities far in excess of what would be expected. The observations made by ground based millimeter instruments, Penfield et al. (1976) indicate an early morning decrease by a factor of 2 between 50 and 60 km, but all these measurements have a high degree of uncertainty. Hays and Roble (1973), using stellar occultation techniques observed values of the ozone density in the mesosphere at night which were lower than the daytime values. Certainly a tenfold increase at 60 km is impossible otherwise we would expect a far greater dispersion of the observational results at this altitude than is found. Until there have been many more

observations, the theoretical model used here for the diurnal changes, is the best that can be devised.

6. Conclusions

Ozone densities have been well documented for the stratosphere with respect to latitudinal dependence for many years and the model given here does not represent a very large improvement on previous models. However in the mesosphere the situation is drastically different and this report has attempted to arrive at a global model for the ozone on poorly distributed and for the most part non-systematic measurements. The model derived here is the best that can be done with the existing data and is open to modification when more accurate and extensive results are available. What is required ideally is a satellite survey, well distributed in latitude and longitude, that is able to use a variety of techniques which could measure ozone densities during the day and night. Failing this, a more systematic approach by rockets, such as that by Watanabe and Tohmatsu (1976), is recommended with results and standard deviations from the mean tabulated rather than presenting the results in graphical form with logarithmic scales which often introduce considerable errors in the reading stage necessary for any collation of data from more than one source.

Acknowledgements.

I would like to thank Prof. G. V. Groves for his encouragement and many useful suggestions. Sponsorship has been provided by the Air Force Geophysics Laboratory (AFGL), United States Air Force under Grant No. AFOSR-77-3224.

References

Anderson, G. P., C. A. Barth, F. Cayla, and J. London, 1969 Ann. Geophys. 25, 341-345.

Carver, J. H., B. H. Horton, R. S. O'Brien, and B. Rofe, 1972 Planet. Space Sci. 20, 217-223.

Dütsch, H. U., 1964 Uniform Evaluation of Umkehr Observations from the World Ozone Network. Pt III., World-wide Ozone distributions at Different Levels and its Variation with Season with 'Umkehr' Observations. National Centre for Atmosphere Research, Boulder Colorado.

Dütsch, H. U., P. Boller, and Ch. Ling, 1969 Ann. Geophys. 25, 215-218.

Dütsch, H. U., and Ch. Ling, 1969 Ann. Geophys. 25, 211-214.

Dütsch, H. U., 1974 Can. J. Chem. 52, 1491-1504.

Evans, W. F. J., E. J. Llewellyn, 1972 Radio Sci. 7, 45-50.

Evans, W. F. J., E. J. Llewellyn, 1969 Ann. Geophys. 26, 167-178.

Hays, P. B., and R. G. Noble, 1973 Planet. Space Sci. 21, 273-279.

Hilsenrath, E., 1969 J. Geophys. Res. 74, 6873-6880.

Johnson, F. S., J. D. Purcell, and R. Tousey, Studies of the Ozone layer above New Mexico. Rocket Exploration of the Upper Atmosphere. Pergamon, London. 1954., ed. R. F. L. Boyd.

Khrugian, A. Kh., The Physics of Atmospheric Ozone. J. Wiley and sons 1975.

Krueger, A. J., 1973 Pure and App. Geophys. 106-108, 1272-1280.

Krueger, A. J., D. F. Heath, and C. L. Mateer, 1973 Pure and App. Geophys. 106-108, 1254-1265.

Kulkarni, R. N., 1962 Quart. J. R. Met. Soc. 88, 522-534.

London, J., and J. E. Frederick, 1977 J. Geophys. Res. 82, 2543-2556.

Manabe, S., and F. Moller, 1961 Monthly Weather Rev. 89, 503-532.

Mani, A., and C. R. Sreedharan, 1973 Pure and App. Geophys. 106-108, 1180-1191.

Miller, D. E., and P. Ryder, 1973 Planet. Space Sci. 21, 963-970.

Nagata, T., T. Tohmatsu, and T. Ogawa, 1970 Space Res. 11, 849-855.

Nicolet, M., 1969 Anns. Geophys. 25, 531-546.

Park, J. H., and J. London, 1974 J. Atmos. Sci. 31,1898-1916.

Penfield, H., M. M. Litvak, C. A. Gottlieb, and A. E. Lilley, 1976 J. Geophys. Res. 81, 6115-6120.

Rawcliffe, R. D., G. E. Meloy, R. M. Friedman, and E. H. Rogers, 1963 J. Geophys.Res. 68,6425-6429.

Riegler, G. R., J. F. Drake, S. C. Liu, and R. J. Cicerone, 1976 J. Geophys. Res. 81, 4997-5001.

Tonsberg, E., and E. L. Olsen, 1943 Geophysiske Publikasjoner, 13, No. 12.

Watanabe, T., and T. Tohmatsu, 1976 Report of Ionosphere and Space Res. 30, 47-50.

Weeks, L. H., R. S. Cuikay, and J. R. Corbin, 1972 J. Atmos. Sci. 29, 1138-1142.

Ozone Data for the World, Dept. of Transport, Meteorological Branch, Toronto, Canada. 1973-1976, Vols. 14-17.

	January					July			
H km	60 N	45	30	15	0	15	30	45	60 N
10	2.95	2.40	1.35	0.62	0.45	0.46	0.77	1.80	2.60
15	3.60	2.60	1.25	0.40	0.27	0.30	0.74	1.80	2.65
20	4.80	3.55	2.50	1.75	1.43	1.95	2.75	3.65	4.16
25	3.60	4.53	4.20	4.02	4.33	4.52	4.55	4.25	3.85
30	2.20	2.65	3.05	3.50	3.80	3.76	3.30	2.80	2.30
35	1.203	1.37	1.50	1.573	1.663	1.712	1.62	1.451	1.201
40	0.628	0.617	0.572	0.525	0.532	0.565	0.574	0.541	0.468
45	0.275	0.236	0.192	0.164	0.156	0.161	0.167	0.163	0.150
50	.0941	.0802	.0656	.0557	.0504	.0494	.0506	.0512	.0510
55	.0293	.0280	.0248	.0217	.0189	.0174	.0170	.0171	.0167
60	.0106	.0103	.00951	.00853	.00748	.00656	.00579	.00503	.00420
65	.00364	.00336	.00303	.00268	.00231	.00194	.00158	.00117	.00081
70	.00089	.00078	.00069	.00060	.00052	.00043	.00035	.00025	.00017
75	.00018	.00017	.00015	.00014	.00012	.00011	.00009	.000075	.00006

	April					October			
H km	60 N	45	30	15	0	15	30	45	60 N
10	3.30	2.75	1.07	0.77	0.73	0.80	1.00	1.40	1.80
15	4.10	3.15	1.50	0.65	0.55	0.40	0.86	1.78	2.55
20	5.00	4.50	3.30	2.40	2.30	2.30	2.40	3.25	4.10
25	4.20	4.60	4.47	4.32	4.30	4.30	4.32	4.00	3.65
30	2.90	2.95	3.08	3.18	3.25	3.0	3.20	2.85	2.30
35	1.407	1.585	1.645	1.495	1.420	1.402	1.568	1.565	1.346
40	0.543	0.636	0.628	0.511	0.461	0.486	0.568	0.661	0.674
45	0.192	0.204	0.190	0.155	0.143	0.152	0.179	0.223	0.262
50	.0653	.0637	.0602	.0549	.0531	.0544	.0588	.0650	.0735
55	.0215	.0212	.0214	.0214	.0212	.0210	.0197	.0182	.0165
60	.00690	.00794	.00882	.00950	.00957	.00895	.00733	.00568	.00360
65	.00221	.00280	.00321	.00357	.00359	.00322	.00259	.00189	.00091
70	.00058	.00068	.00075	.00080	.00080	.00073	.00063	.00050	.00029
75	.00016	.00015	.00015	.000145	.00014	.000135	.00013	.000125	.00012

Table 1.

The ozone number density in units of 10^{12} mols. cm^{-3} for the months January, July, April and October, for latitudes 0 - 60 N and heights 10 - 75 km.

Time.	Height km. 50	55	60	65	70	75
0	1.0	0.955	0.776	0.436	0.309	0.115
1	1.0	0.955	0.891	0.537	0.407	0.178
2	1.0	0.977	0.851	0.589	0.501	0.295
3	1.0	0.977	0.891	0.661	0.575	0.389
4	1.0	0.977	0.912	0.708	0.631	0.525
5	1.0	0.977	0.933	0.813	0.741	0.661
6	1.0	0.977	0.955	0.851	0.813	0.794
7	1.0	0.977	0.891	0.871	0.912	0.549
8	1.0	0.977	1.0	0.933	0.955	0.933
9	1.0	0.977	1.0	0.955	0.955	0.977
10	1.0	0.977	1.0	0.977	1.0	1.0
11	1.0	0.977	1.0	1.0	1.0	1.0
12	1.0	0.977	1.0	1.0	1.0	0.977
13	1.0	1.0	1.0	1.0	0.977	0.955
14	1.0	1.0	1.0	1.0	0.955	0.912
15	1.0	1.0	0.977	1.0	0.912	0.851
16	1.0	1.0	0.955	0.933	0.813	0.759
17	1.0	1.0	0.912	0.832	0.708	0.661
18	0.977	0.977	0.871	0.741	0.631	0.525
19	0.955	0.977	0.891	0.741	0.501	0.398
20	0.933	0.933	0.912	0.776	0.417	0.389

Table 2.

The diurnal multiplication factors for the mesospheric ozone model. Column 1 gives the time in twentieths of the interval between sunrise and sunset.

Key to figures 1-28

Symbol	Instument/technique	Measurement made from	Author (date)
O	B.U.V. Spectrometer	Nimbus satellite	Krueger et al.(1973)
	U.V. Radiometer	Rocket	Watanabe and Tohmatsu (1976)
and 	B.U.V. Spectrometer	Ogo satellite	London et al. (1977)
●	Solar spectrometer	Rocket	Johnsor (1952)
	B.U.V. Spectrometer	Satellite	Anderson et al. (1969)
	U.V. Spectrometer	Rocket	Nagata et al. (1970)
	U.V. Spectrometer	Rocket	Miller and Ryder (1973)
◊	1.27μ Airglow emission	Ground	Evans and Llewellyn (1969)
	Chemiluminescent detector	Parachute	Hilsenrath (1969)
■	Millimeter wave	Ground	Penfield et al. (1976)
K	Arcas optical ozonosonde	Rocket	Krueger (1973)
	U.V. Radiometer	Satellite	Rawcliffe et al. (1963)
	U.V. Photometer	Rocket	Weeks et al. (1972)
	U.V. Spectrometer	Satellite	D. E. Miller (Private communication)
x	Electrochemical sonde	Balloon	Mani and Streedharan (1973)
	Theoretical	N.A.	Parks and London (1974)
R	Not known	Rocket	D. E. Miller (Private communication)
	Umkehr	Ground	N.A.

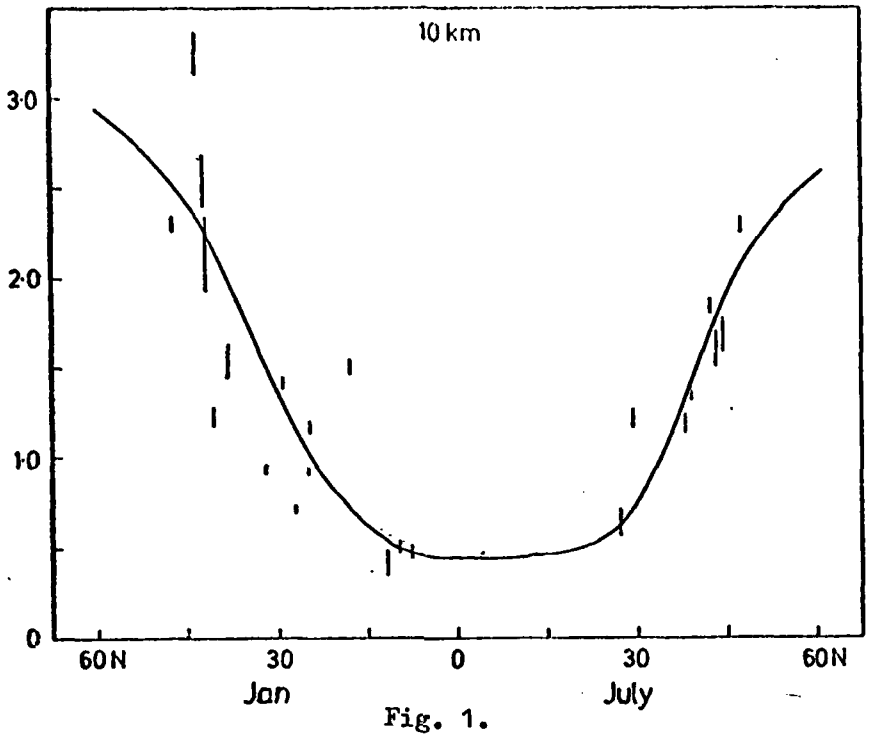

Fig. 1.

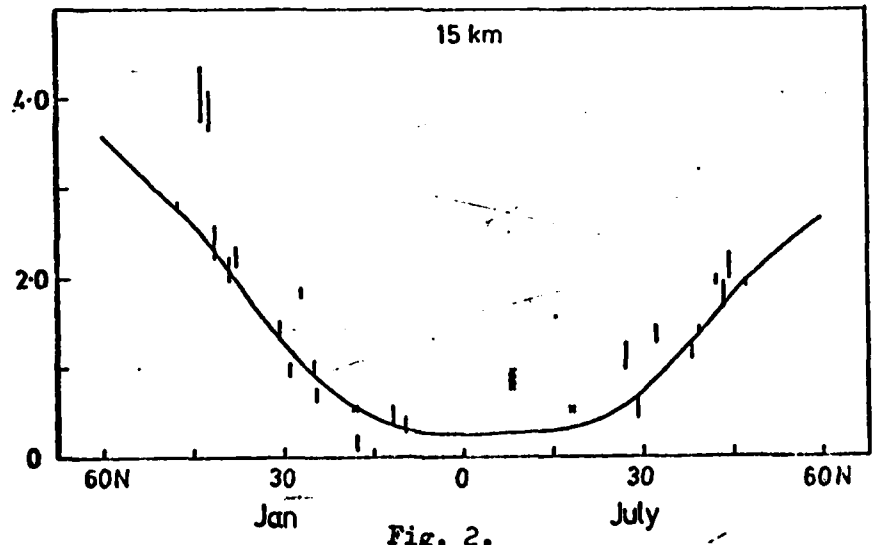

Fig. 2.

$O_3 \times 10^{12}$ mols/cm^3

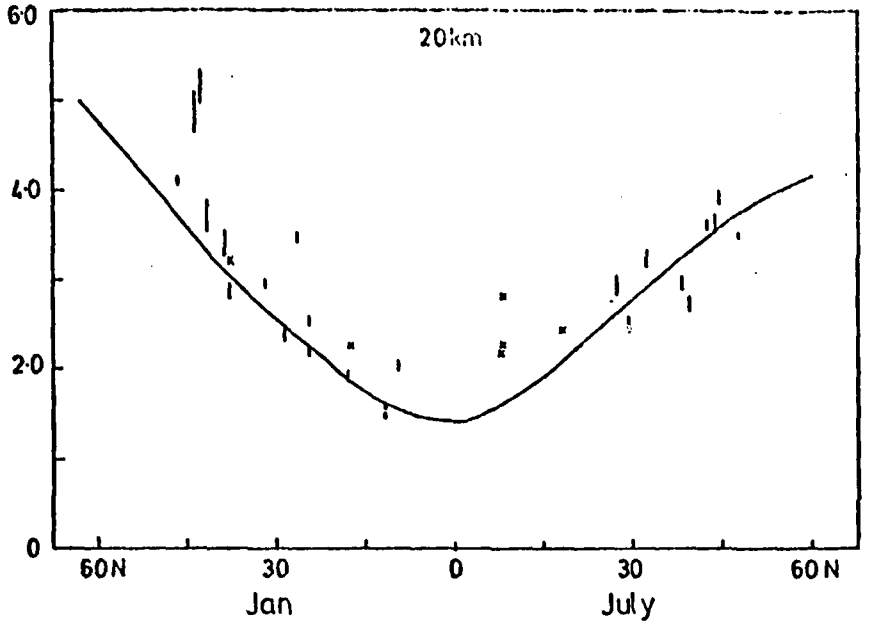
20km
6·0
4·0
2·0
0
60N
30
0
30
60N
Jan
July

Fig. 3.

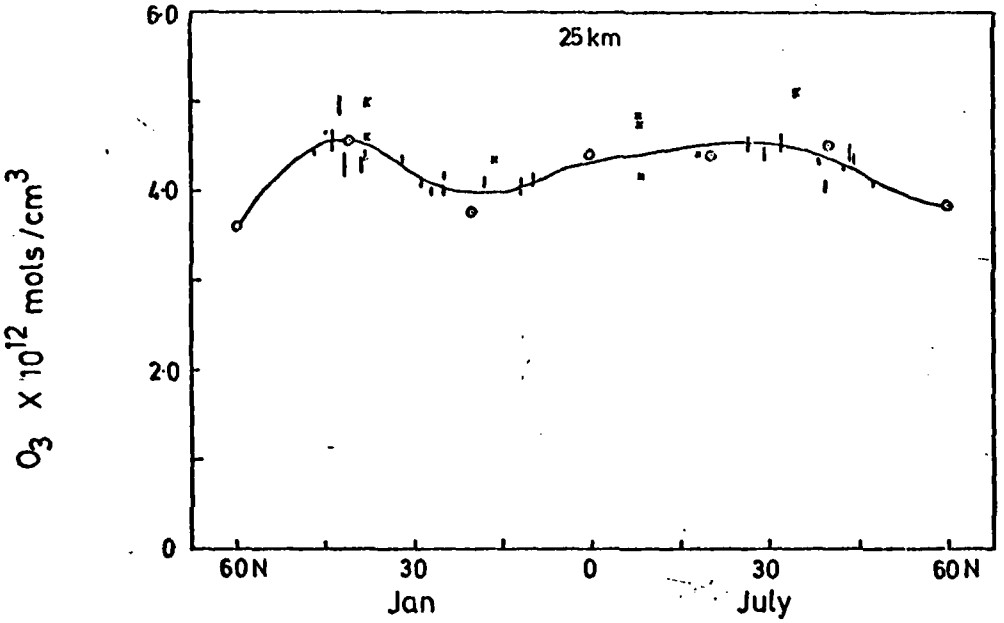
25km
6·0
4·0
2·0
0
60N
30
0
30
60N
Jan
July
O_3 X 10^{12} mols/cm^3

Fig. 4.

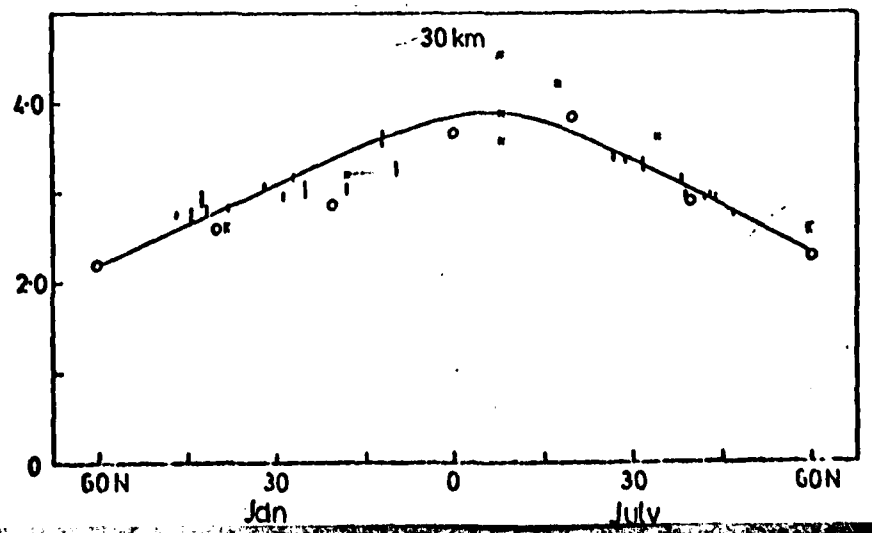
30km
4·0
2·0
0
60N
30
0
30
60N
Jan
July

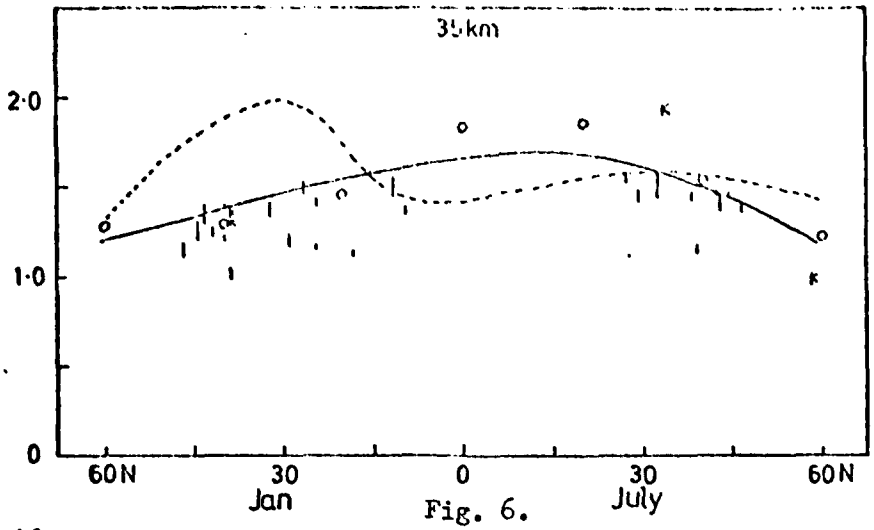

Fig. 6.

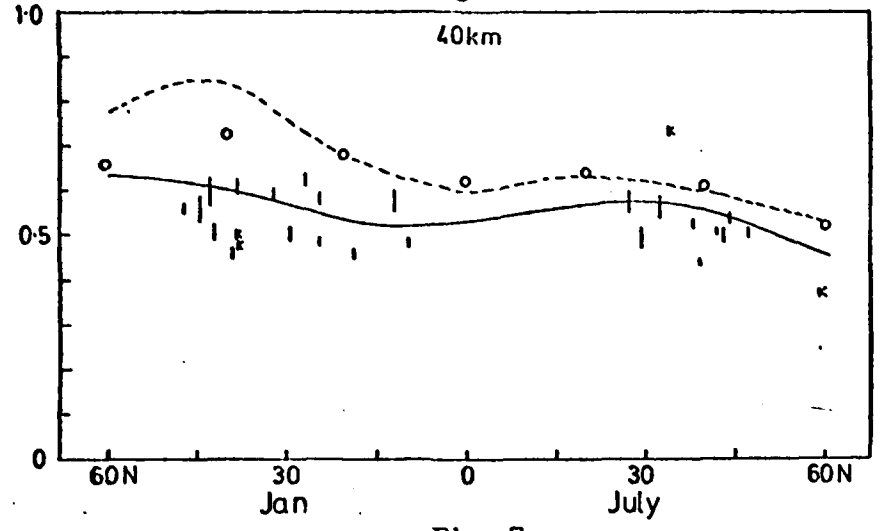

$O_3 \times 10^{12}$ mols/cm^3

Fig. 7.

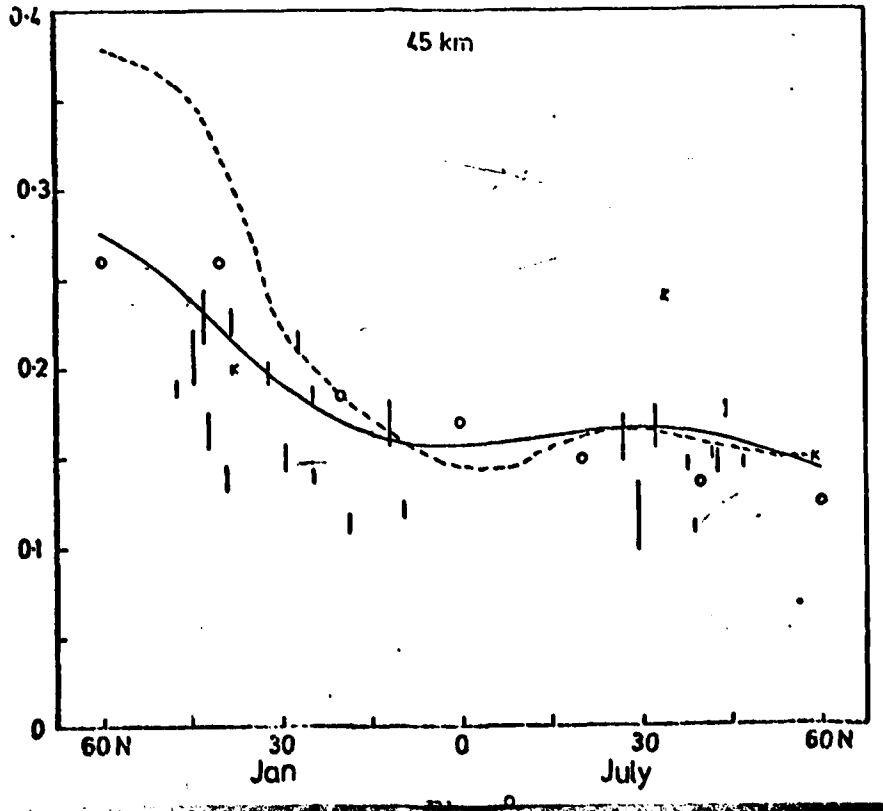

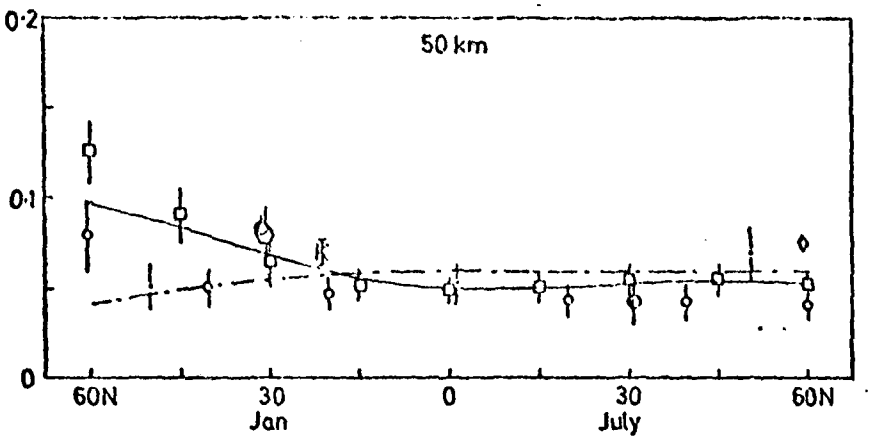

Fig. 9.

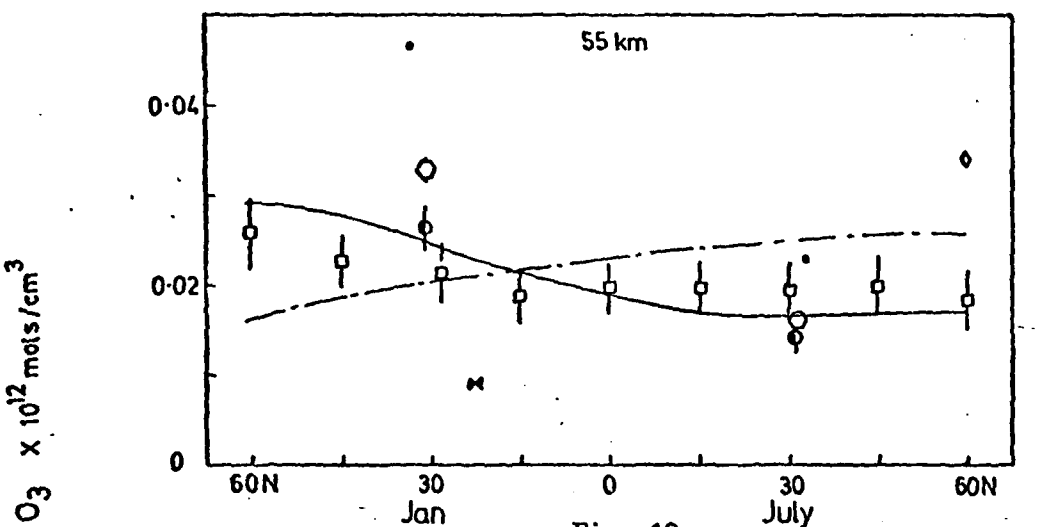

Fig. 10.

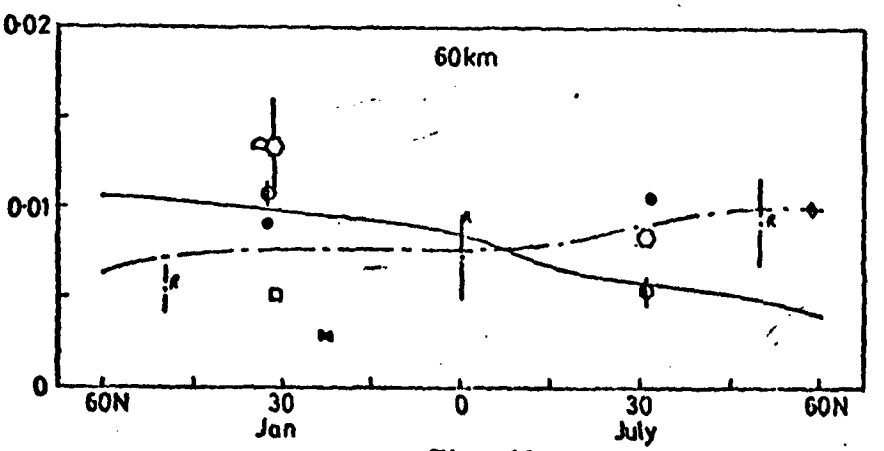

Fig. 11.

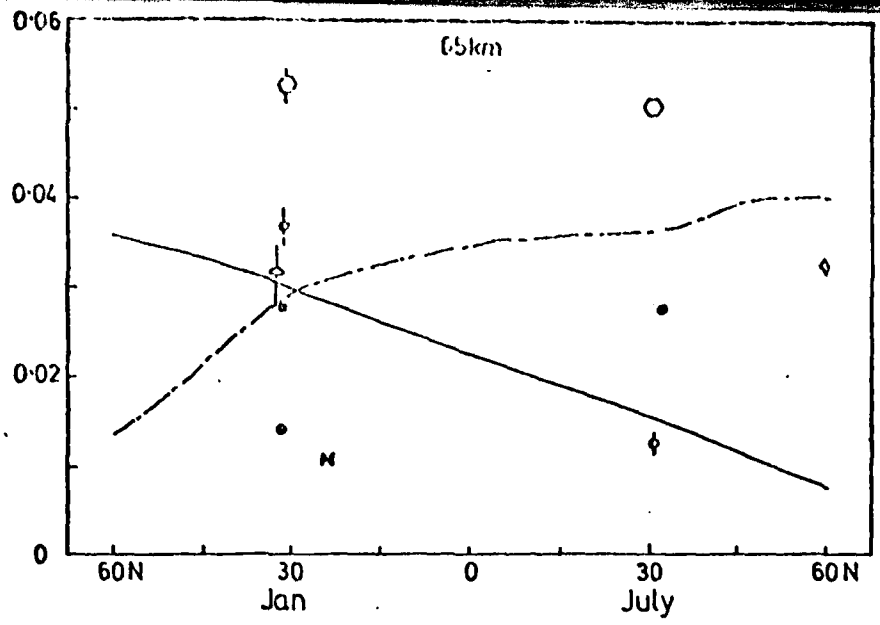

Fig. 12.

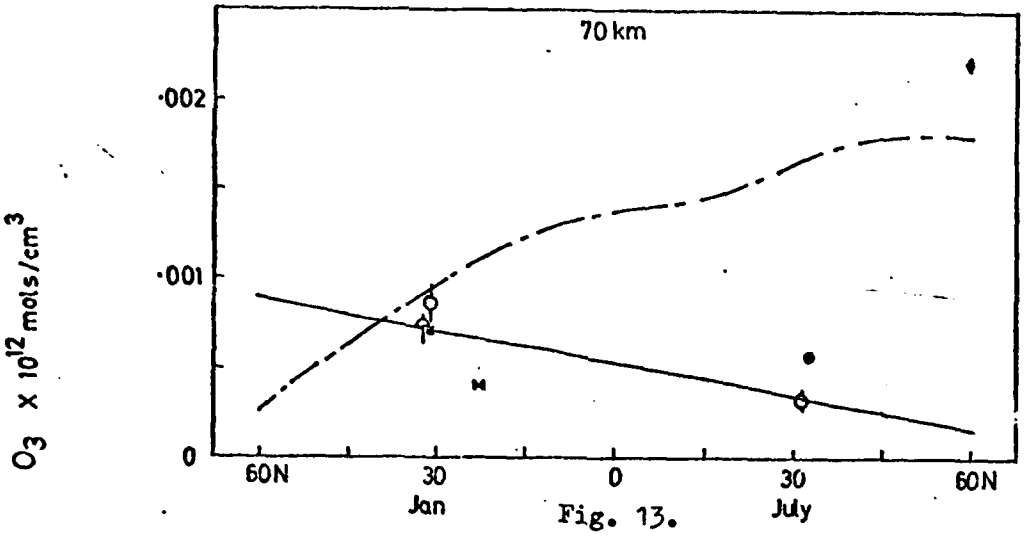

Fig. 13.

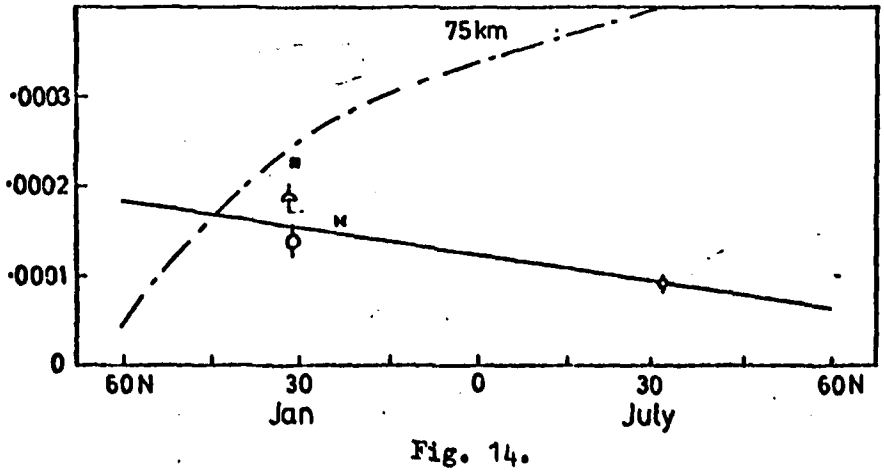

Fig. 14.

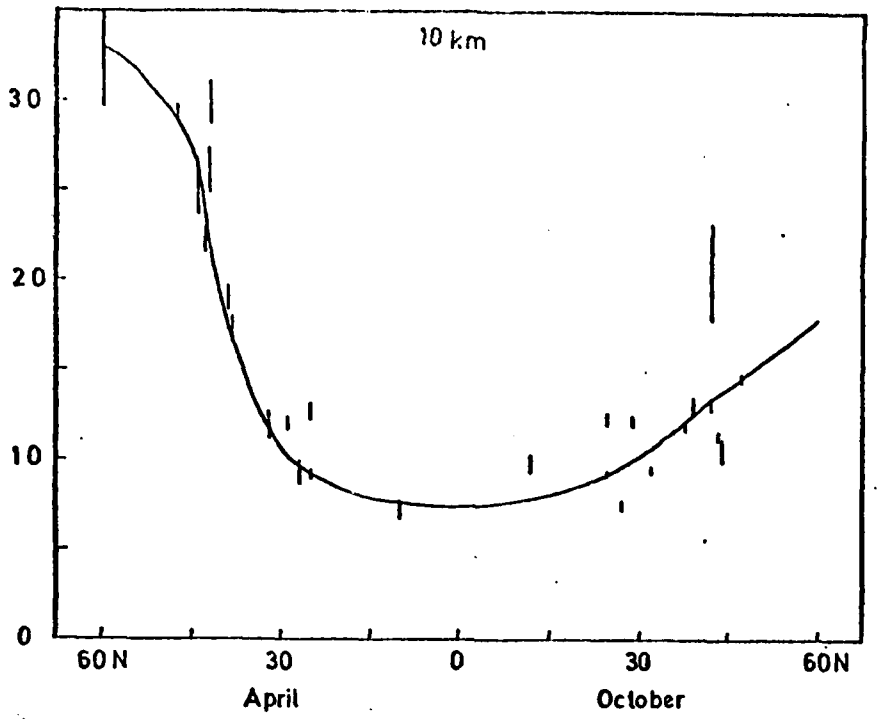

Fig. 15.

$O_3 \times 10^{12}$ mols/cm^3

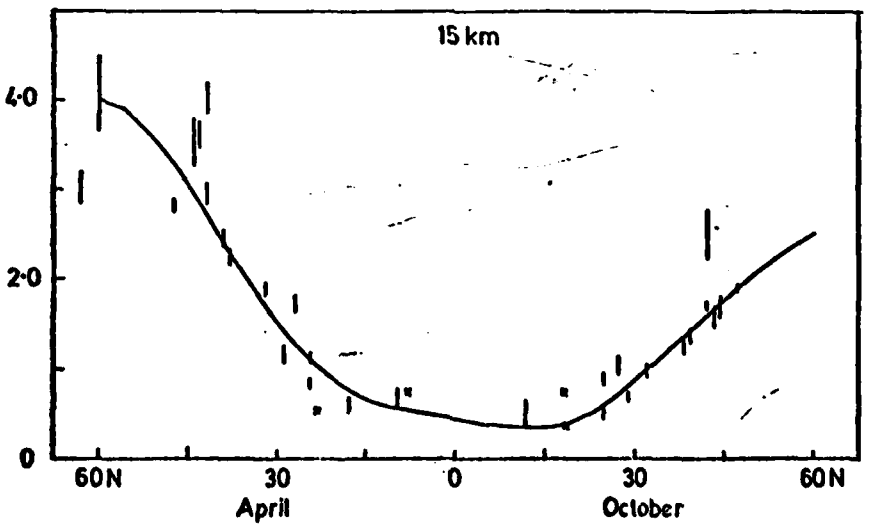

Fig. 16.

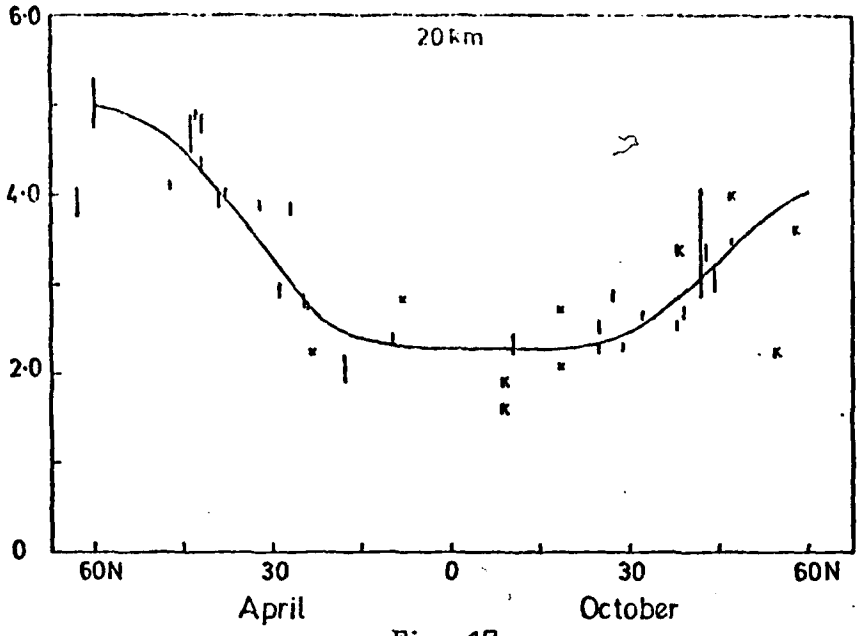

Fig. 17.

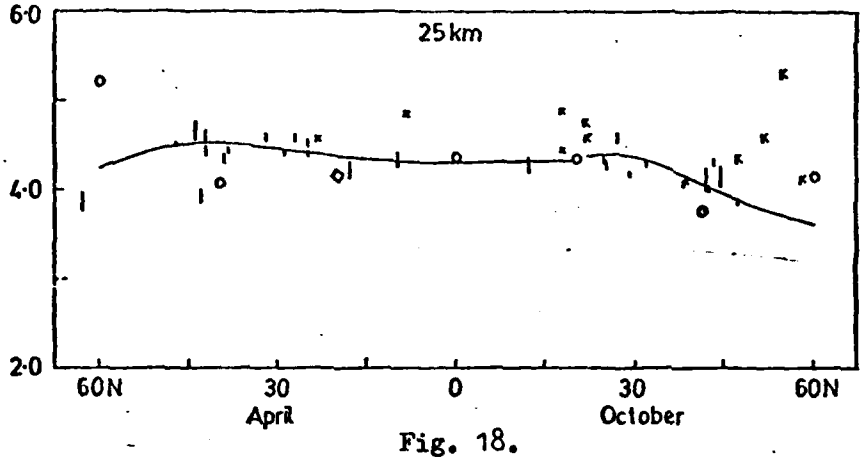

$O_3 \times 10^{12}$ mols/cm^3

Fig. 18.

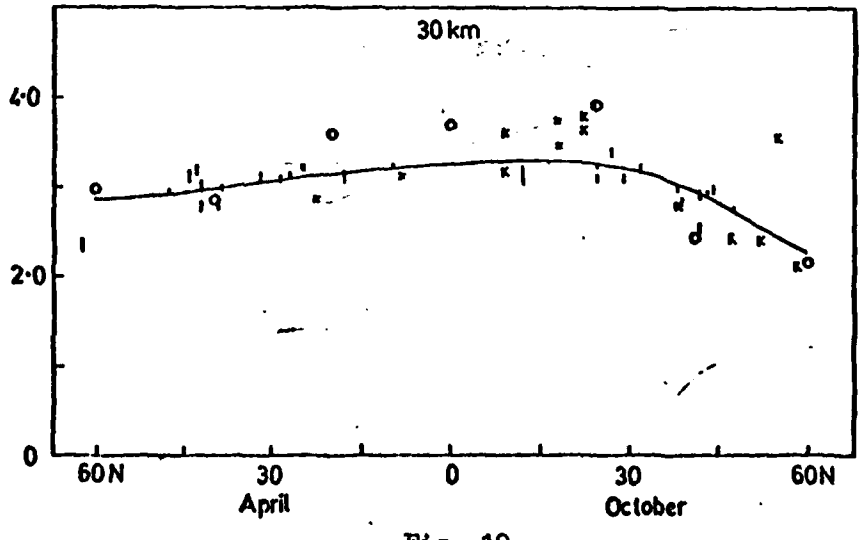

Fig. 19.

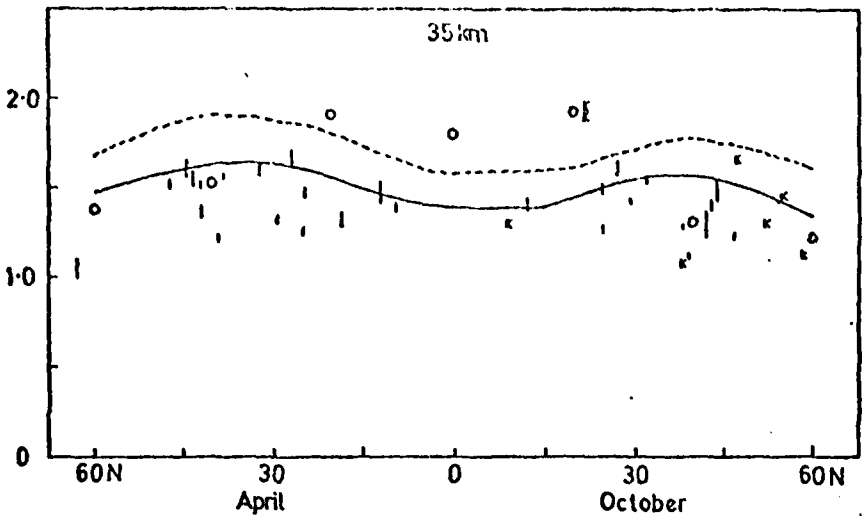

Fig. 20.

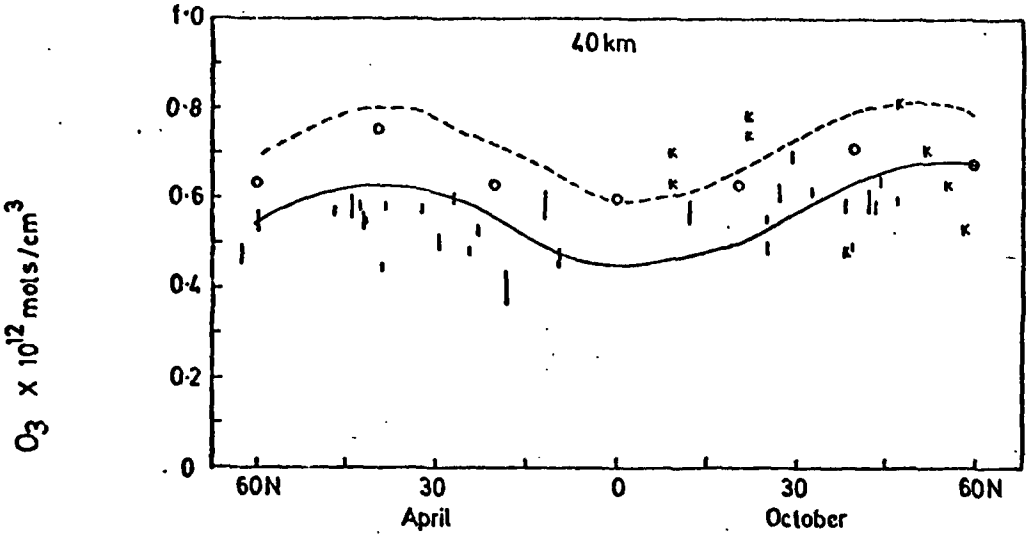

Fig. 21.

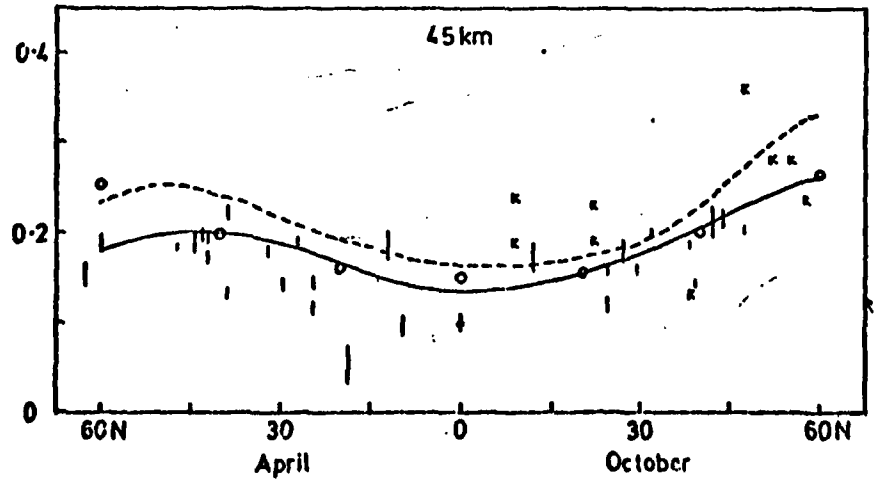

Fig. 22.

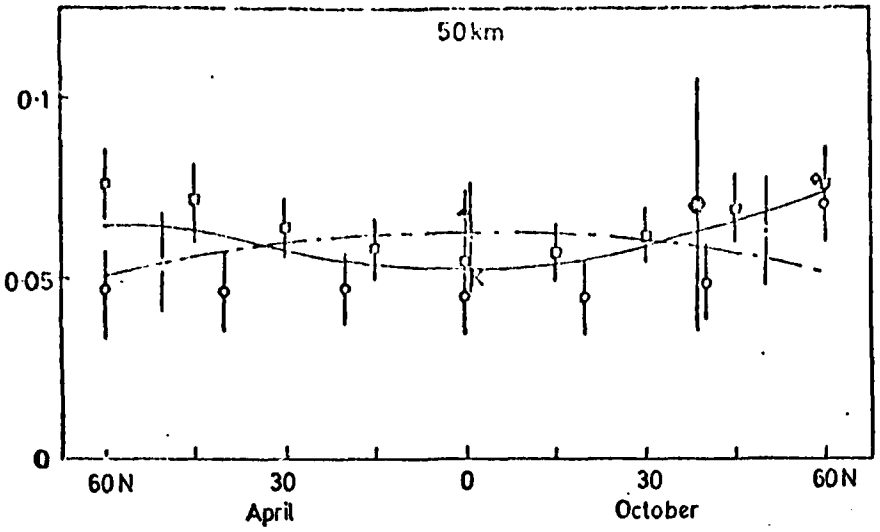

Fig. 23.

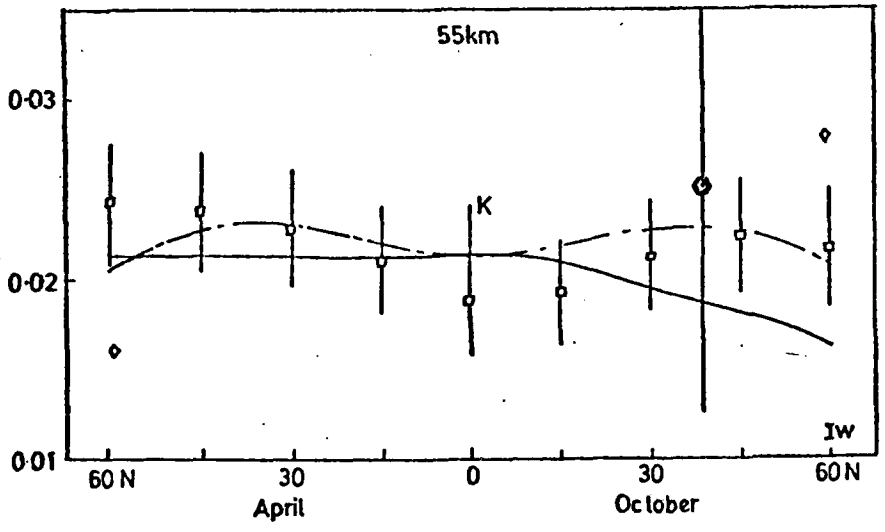

$O_3 \times 10^{12}$ mols/cm^3

Fig. 24.

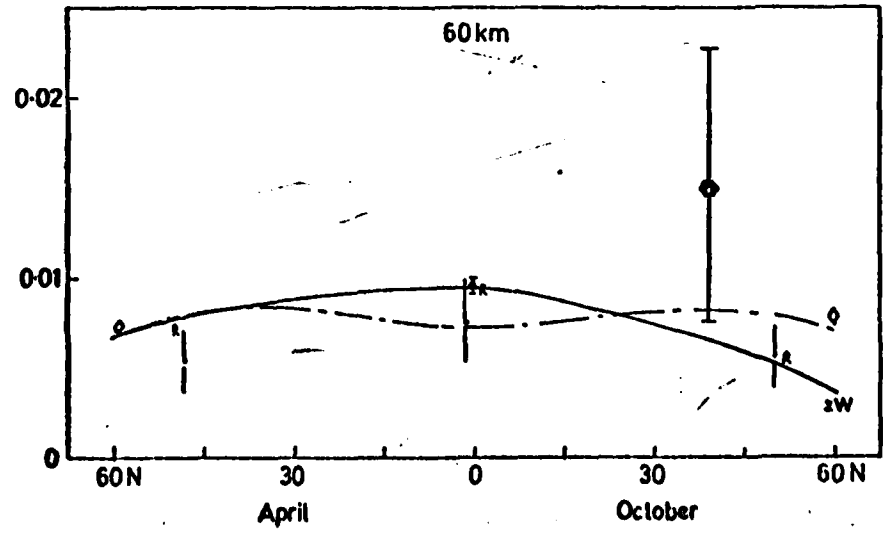

Fig. 25.

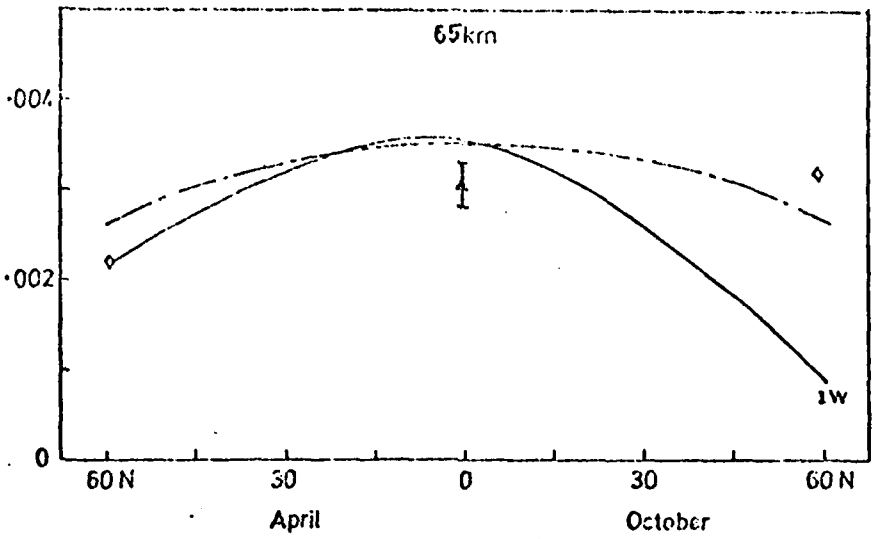

Fig. 26.

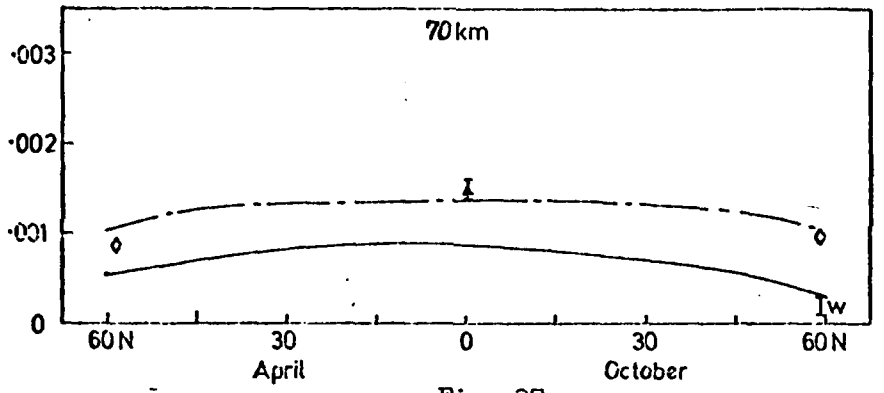

$O_3 \times 10^{12}$ mols/cm^3

Fig. 27.

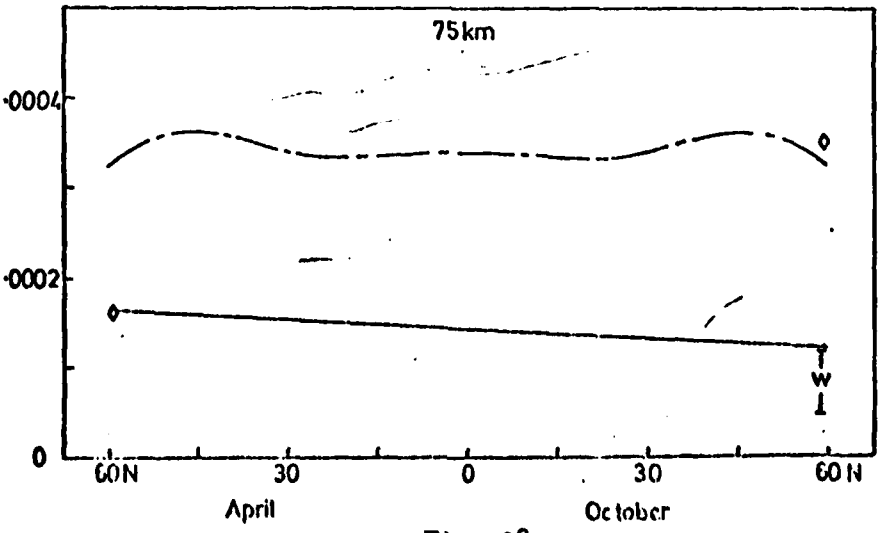

Fig. 28.

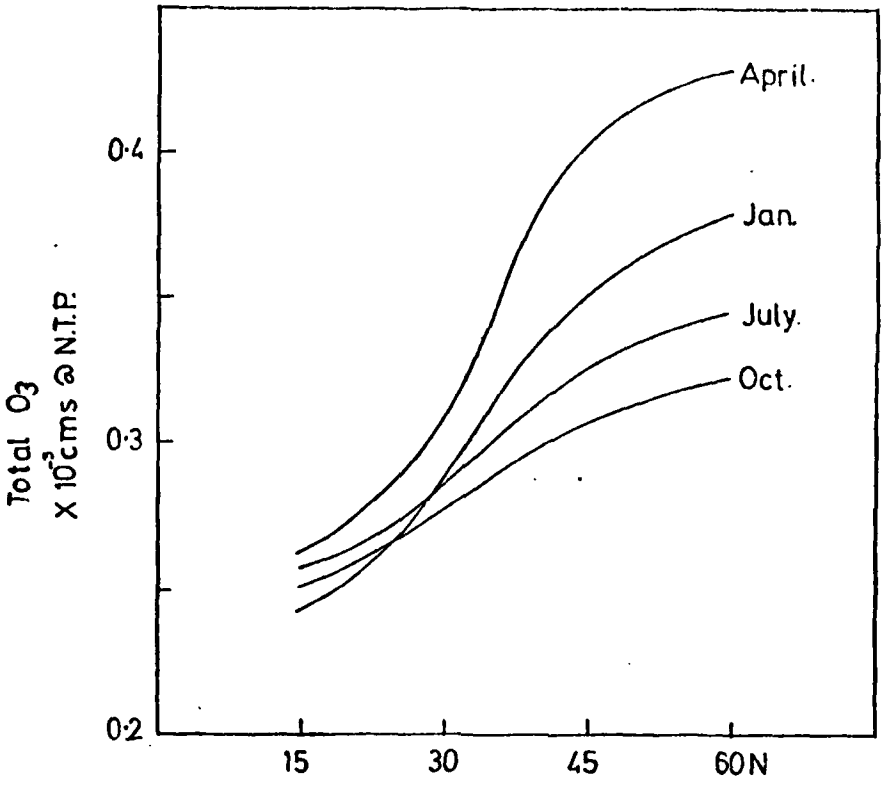
April
Jan.
July
Oct.
0·4
0·3
0·2
Total O_3
X 10^{-3}cms @ N.T.P.
15
30
45
60N

Fig. 29

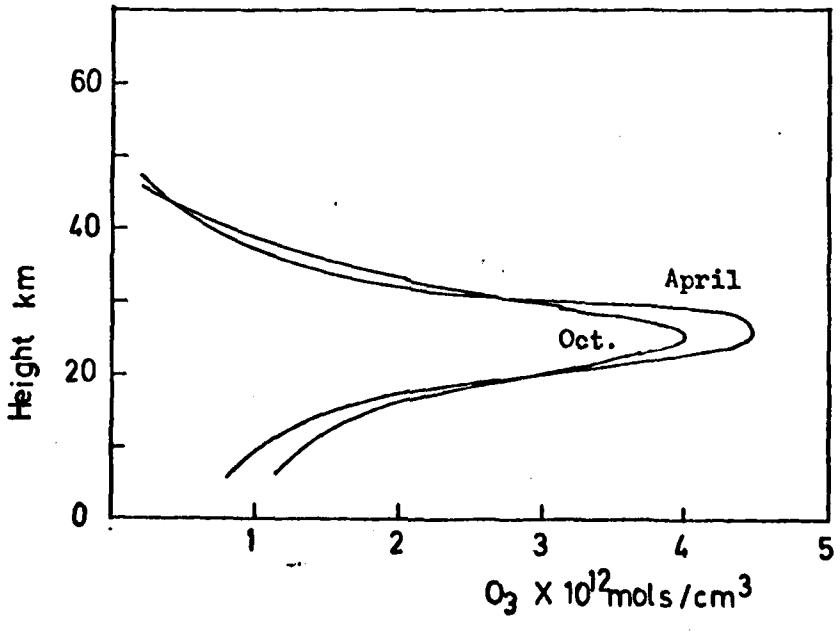
60
40
20
0
Height km
April
Oct.
1
2
3
4
5
O_3 X 10^{12}mols/cm^3

Fig. 30

Seasonal and diurnal variations of middle atmosphere winds

G.V. Groves

Department of Physics and Astronomy, University College London

Presented at the Discussion Meeting of the Royal Society on 'The Middle Atmosphere as observed from Balloons, Rockets and Satellites', 12-13 December 1978

ABSTRACT

Previously published meridional cross-sections of monthly mean W-E and S-N wind components from 60 to 130 km are reviewed in the light of wind data obtained by ground-based radio methods over various time scales including that of the solar cycle. A mean meridional circulation in the winter hemisphere is inferred in which a dominant mesospheric cell between low and high latitudes is confined to lower heights at higher latitudes: a second meridional circulation is tentatively located above the former in the lower thermosphere extending downwards to lower heights at higher latitudes and introducing the possibility of polar and equatorial air mixing at mid-latitudes at heights close to 90 km. Meridional circulation is discussed in relation to the winter anomaly in D-region radio-wave absorption.

Diurnal and semidiurnal wind oscillations at heights between 25 and 60 km are presented which are the results of a comprehensive analysis of data from short series of rocket launchings held at various western hemisphere sites between 1965 and 1974. Phase and amplitude profiles at different times and locations rarely show similarities, but at latitudes greater than about 30° S-N components are consistently in quadrature with and similar to the W-E components. An interpretation of the oscillations at these latitudes in terms of a superposition of tidal modes indicates the presence of quasi-steady high-order modes excited at tropospheric heights by sources of limited ($\sim 10^3$ km) extent. At latitudes less than about 30°, steady or quasi-steady diurnal and semi-diurnal components are not necessarily the dominant components of daily variation. At high latitudes diurnal phases generally show little change with height in comparison with observations at lower latitudes in accord with the latitudinal properties of positive and negative diurnal modes.

1. Introduction

Since the early 1950's and particularly during the 1960's rocket techniques have provided a major source of new information on upper atmosphere structure. The role of the rocket in this type of experimentation has usually been that of a vehicle of transport from which to eject one or more types of experimental package in flight. Data have been acquired for different height regions by means of parachutes or similar forms of decelerating device (often with a temperature sensing package) as well as chaff, falling spheres, grenades and chemical releases. Atmospheric temperatures, pressures and densities have been investigated by these techniques, but the parameter most frequently measured over different height intervals extending into the thermosphere has been the wind velocity.

At heights close to 90 km ground-based radio techniques have also been available for wind determination. Although their observational height range is of limited extent compared with that of rocket techniques, they are particularly suitable for the study of time dependences which in upper atmosphere winds are traditionally classified in terms of a prevailing component, being that part of the wind velocity that does not change in the course of a day, tidal motions, turbulence and gravity waves of a few hours periodicity or less. Seasonal and longer-term effects contribute to the prevailing component but in addition day-to-day variations (of about 4 days periodicity) have also been found to contribute significant energy peaks to the spectra of meteor wind data (Teptin 1972).

In the first part of this paper (§2 to 6) seasonal wind variations at heights above 60 km are reviewed particular attention being given to S-N components and meridional circulation. The second part of the paper deals with diurnal wind variations as investigated by short series of rocket launchings extending over 1 to 3 days at heights of 25 to 60 km (or to 90km on a few occasions). On 19-20 March 1974 70 rockets were launched

at 8 western hemisphere sites; and the results from these launchings are presented and discussed in §§ 7 to 13 in conjunction with those of earlier launchings.

2. Meridional cross-sections of W-E and S-N winds, 60-130 km

The smaller types of meteorological rocket that are in regular use with for example the U.S. Meteorological Rocket Network rarely contribute wind data above 60-70 km altitude and it is therefore upon the relatively fewer launchings of medium-sized vehicles that data acquisition at these heights has depended. In relation to the complex nature of wind variations in space and time, coverage has been extremely sparse. Nevertheless it has been possible by combining rocket data (and gun-probe data at certain sites) with radio wind data to construct meridional cross-sections of mean W-E and S-N wind components at monthly intervals (Groves 1969). The rocket and gun-probe data available at that time were from grenade experiments at Woomera, Wallops Island and Fort Churchill and chemical releases at Barbados, Eglin, Woomera and other mid-latitude sites. Data were provided by ground-based radio techniques sited in Europe and the S hemisphere at Adelaide and at Mawson.

Figure 1 shows the models for 1 January. In constructing these cross-sections seasonal symmetry was assumed between N and S hemispheres in an attempt to overcome the shortage of data, i.e. S hemisphere data were combined with N hemisphere data after a six-month change of date and a change of sign of S-N components. On account of the poor longitudinal distribution of data and unknown magnitude of standing waves, the extent to which the models represented zonal mean values was uncertain; values of 20 m/s for S-N wind components at 90 km being considered to be unlikely to be globally representative. As cross-sections of observed averages however the models provided a convenient reference against which to compare other individual measurements that might become available. The W-E wind model in a slightly revised form was included in CIRA 1972, Part 2.

3. Comparisons of recent radio wind data with S-N and W-E models

In recent years a number of comparisons have been made between radio wind observations and the S-N and W-E models of § 2. Many of these observations are from longitudes where data were not previously available, notably in the western hemisphere, and offer the opportunity of checking the main features of the models and their seasonal trends for a range of heights centred close to 90 km.

The first measurements by partial radiowave reflections at Saskatoon (52°N, 107°W) (Gregory & Rees 1971) showed satisfactory agreement with the 1969 models, but more extensive comparisons up to 110km (Gregory & Manson 1975) have shown satisfactory agreement to 85 km only and differences in the annual variation of zonal flow above 100 km.

Mean meteor winds measured at Durham, New Hampshire (43°N, 71°W) from May to December 1970 were in general agreement with the models, the meridional winds showing equatorwards flow of 10 m/s during summer and a similar poleswards flow in winter (Clark 1975). A similar magnitude of ~10 m/s equatorwards flow in summer (August 9 to September 4 1974) was found for 90-100 km at Atlanta (34°N, 84°W) (Roper 1975).

In 1970, meteor wind data were obtained for the first time in Jamaica (18°N, 77°W) and results from March 1971 to February 1972 (Scholefield & Alleyne 1975) showed a seasonal variation in good agreement with the 1969 models. The general trend of the S-N component (figure 2) was equatorwards in summer and polewards in winter, although data points deviated appreciably from the model at times: the particularly large deviation in March-April 1971 corresponded to replacement of easterly by northerly flow.

Meridional flow from November 1970 to November 1971 in the meteor region at Christchurch, New Zealand (43°S, 72°E) was equatorwards in local summer and polewards in local winter being not in conflict with the pattern of flow suggested by figure 1 (Wilkinson & Baggaley 1975).

Monthly mean ionospheric drifts from 80 to 100 km for 1972 have been obtained at Adelaide (35°S, 139°E) by the partial reflection technique and compared with the 1969 models (Stubbs 1976). Overall, the models provided a better picture of the 1972 winter than the 1972 summer for which they fairly consistently exceeded observed S-N drift velocities and underestimated W-E magnitudes. For 15-21 June 1973 prevailing components have been derived with estimates of error, and S-N components compare well with model values as shown in figure 3 (Vincent & Stubbs 1977).

4. Day-to-day and long-term wind components

The spread of data points in figure 2 is evidence of the presence of variations on time scales of greater than one day and less than a few weeks. Such variations are now recognized as a general feature of radio wind observations with various possible dominating periodicities according to location, altitude and time of year. Spectral analysis of meteor radar winds at Obninsk (55°N, 36°E) and LF radio drift measurements between Kühlungsborn (54°N, 12°E) and Collm (51°N, 13°E) during the period November 1972 to March 1973 show peak intensities at periods of 10-16 days for the zonal, 16-20 days for the meridional component and of 2.5-6 days in both components (Lysenko et al. 1975). The results of other investigators tend to fall in the same ranges. Periods between 2 and 5 days and amplitudes between 10 and 20 m/s were found by Muller & Kingsley (1974) at Sheffield (53°N, 1°W), the absence of a marked seasonal effect being taken to indicate an indirect process of coupling with tropospheric variations of similar periodicities and not direct planetary wave propagation. Simultaneous wind variations at Garchy (47°N, 3°E) and Obninsk have been identified as a planetary wave of a 2-day period and longitudinal wave number around 3 (Glass et al. 1975). At Adelaide (35°S, 139°E) the variation is again found at all times of the year and is comparable in magnitude to that of the mean flow being quasi-periodic with ~10-15 d periods (Elford 1976). Long-period waves also appear in spectral

analyses of data from Durham, New Hampshire (Clark 1975) and Saskatoon (Belmont et al. 1977). The quasi-periodic character of the variations is well illustrated by figure 4 which shows the S-N prevailing wind for winter 1972/3 at Obninsk, the results having been subjected to harmonic analysis with a sliding 24 h interval shifted in steps of 1 h, and at Kühlungsborn-Collm where values refer to midnight (Lysenko et al. 1975).

Long-term variations can be studied at only a few sites which have an adequate time record. During the years 1966 to 1972 meteor winds at Adelaide showed a sudden change in early 1969 of the vertical gradient of the meridional component at 90 km from slightly positive (~+1 m/s/km) to slightly negative (~-1 m/s/km) without evidence of any substantial complementary change in the zonal flow (Elford 1976). From the 1956-73 run of ionospheric drift measurements at Kühlungsborn-Collm an oscillation of about 22 month period in the zonal prevailing wind has been reported (Sprenger et al. 1975). A dependence on solar activity of the prevailing winter-time (November to February) winds was shown some years ago for both W-E and S-N components by the Kühlungsborn-Collm observations (Sprenger & Schminder 1969). This dependence has been confirmed by subsequent data up to 1975 and by the radar meteor wind measurements at Obninsk as shown for the S-N component in figure 5 (Portnjagin et al. 1977). No well-defined correlation between wind speeds and solar activity has been found for summer months.

5. An inferred meridional circulation

Thermally-driven circulations between summer and winter hemispheres were depicted in the two-dimensional theoretical 20-80 km models of Leovy (1964) with meridional winds increasing to 1.8 m/s at 70 km. This pattern of interhemispheric flow differs from that shown in figure 1

where maximum velocities reach much higher values of 10 to 20 or more m/s close to 95 km and the latitudinal dependence is not that of a simple interhemispheric circulation cell. Subsequent radio wind measurements (§3) have provided further evidence of the higher values of S-N velocities shown by the model in the region of 90 km at the solstices; and as many of these observations are at new longitudes model values now appear unlikely to be greatly in excess of zonally-averaged means. If such is the case a mean meridional circulation may be derived on the basis of the S-N and W-E monthly wind models.

The problem has already been investigated at heights between 70 and 100 km by Ebel (1974) who used the steady state equations and the 1969 models to calculate the corresponding mean vertical motion (along with the required heat and momentum sources). The results obtained for equinox and solstice conditions show that the strength and direction of the circulation cells undergo a marked annual change. During the equinoxes the circulation is predominantly symmetric with respect to the equator having 4 cells pole-to-pole. At the solstices it is strongly asymmetric with 5 cells pole-to-pole (reducing to 3 at the lower heights considered) and this circulation appears to be superimposed on a single-cell pole-to-pole circulation of the type proposed by Kellogg (1961). For winter the calculations depict upward motion between 5° and 20° latitude at all heights considered (figure 6): downward motion is obtained between 30° and a higher latitude which is about 50° for the upper half of the 70-100 km altitude range increasing to close to 90° latitude at 70 km. In other words, the mesospheric circulation cell over the winter hemisphere involves air rising at low latitudes, merging with a small interhemispheric flow and descending as it moves towards the winter pole.

The equatorwards flow at 60-65 km in the S-N model of

figure 1 is indicative of a closed or nearly closed circulation in which descending polar air turns equatorwards. The upper boundary of this circulation cell is the zero S-N velocity line in figure 1 which passes through 80 km altitude at 80° latitude and slopes upwards to 111 km at 20° latitude: the gradient of the line is about 1:200. On its upper side the flow reverses reaching high equatorwards velocities at 120 km (figure 1). No calculations of vertical motion are available at these heights and nothing definite can be said about the lower thermosphere circulation, but it may be noted that the equatorwards flow of the model would be consistent with a circulation in which air descends over the winter polar region and ascends at low latitudes. A tentative picture that may therefore be presented of the winter hemisphere meridional circulation is that of two separate but likewise rotating circulations one in the mesosphere and one in the lower thermosphere. Their common boundary on average is represented by the sloping zero S-N line of figure 1, which is the dividing line between two contrary moving air streams one originating at high latitudes and one at low latitudes. At 90-95 km altitude and equatorwards of mid-latitudes the circulation is within the uppermost part of the mesospheric cell, whereas polewards of mid-latitudes at these heights the circulation is within the lowermost part of the thermospheric cell.

The proximity of two contrary flow regions invites consideration of the extent to which they mix and of possible aeronomic consequences. While these matters lie beyond the scope of this paper, attention is drawn to the possible contribution of horizontal as well as vertical turbulent mixing. The presence of small-scale turbulent motions is well established for the 85-105 km region, but the day-to-day variations such as those apparent in figure 4 would effect horizontal transport of air with path lengths

of the order of 1000 km and may be responsible for large-scale eddy mixing. On such time scales horizontal displacements across a zero S-N velocity line in figure 1 are of course possible as figure 1 represents the monthly mean situation.

6. Meridional circulation and the winter anomaly

The striking correlations that have been observed between the winter anomaly in D-region radio-wave absorption and meteorological parameters such as stratospheric temperatures point to atmospheric circulation as being relevant to the ionospheric phenomenon. As the latter in its most conspicuous form consists of days or groups of days of excessive absorption any relationship with meteorological parameters would more reasonably be strongest with departures from the average than with the average itself. A number of physical processes are likely to be involved in establishing the internal atmospheric conditions appropriate to anomalous absorption and here we consider only the meridional circulation as a contributing effect. In this case absorption would be expected to correlate significantly with S-N wind components in any set of observational data.

The winter observations at Arenosillo (37°N, 7°W) of 1969-70 showed that absorption increased with increasing winds from southern directions at 85 km and with increasing winds from northern directions between 90 and 93 km (Rose *et al.* 1972a). Considered in conjunction with figure 1, these results would indicate an increase in mass flow above and below the zero S-N velocity line at times of greater absorption with the upper cell extending downwards to possibly 10 km below its normal position.

The absence of the winter anomaly south of about 30° latitude directs attention to the latitudinal form of the meridional circulation at the altitude of the anomalous absorption which is typically close to 84-85 km (Laštovička 1972). On moving from mid to low latitudes

in the winter hemisphere a number of changes in the meridional circulation occur: S-N wind velocities decrease and the zero S-N velocity line (figure 1) continues to increase in altitude and becomes ill-defined. Ebel (1974) sees the 30° latitude limit as coinciding with the reversal from downward motion at mid-latitudes to upward motion at low latitudes as shown in figure 6.

Although no definite conclusions can be reached at the present stage about the role of the meridional circulation in contributing to the internal atmospheric conditions appropriate to anomalous absorption, it appears worthy of consideration in future investigations.

7. Diurnal launch series 1965-74

Table 1 summaries the sets of data from short series of rocket launchings at different sites whose analysis for diurnal and semidiurnal wind components is presented here. On 19-20 march 1974 70 rockets equipped with standard Datasonde instrumentation were launched at 8 western hemisphere sites by N.A.S.A. Wallops Flight Center in cooperation with other agencies in order to study atmospheric tides and their latitudinal variation (Schmidlin et al. 1975). The locations of the 8 sites are shown in figure 7. Most of the other series of launchings in Table 1 were carried out within the U.S. Meteorological Rocket Network during the years 1965-8, the height range of investigation being approximately 25 to 60 km. The 23-25 October 1968 launchings took place simultaneously at Ascension Island, Cape Kennedy, Fort Churchill and Thule, whereas other launchings were conducted on different dates at various low, mid and high latitude sites. The 24-28 February 1970 launchings were of Skua II rockets carrying a very light-weight chaff to measure winds from about 75 to 95 km altitude over Arenosillo (Rose et al. 1972b). The acoustic-grenade technique provided results to 90 km over Kourou on 19-22 September 1971 (Smith et al. 1974) and the same technique provided results from 24 launchings

at Natal in 1966-68 (Smith et al. 1968, 1969, 1970). Where no specific reference is quoted in the text, the data source has been the Meteorology Data Reports of World Data Center A.

8. Method of harmonic analysis of data

It has been assumed that a wind component v may be represented as a sum of mean, diurnal and semidiurnal components by

$$v = v_o + A_1 \cos\frac{\pi t}{12} + B_1 \sin\frac{\pi t}{12} + A_2 \cos\frac{\pi t}{6} + B_2 \sin\frac{\pi t}{6} \qquad (1)$$

where t is local mean time in hours, departures from apparent local solar time being neglected. v_o, A_1, B_1, A_2, B_2 are five unknowns which may be determined together with estimates of their standard deviations by the method of least squares from, in principle, six or more observations. The analysis has been previously described (Groves 1967) and does not require equal time intervals between observations. All observed wind values have been given an equal weight, although the analysis permits the introduction of different weights.

Results are presented below in terms of the amplitudes and phases of the harmonic components which may be readily calculated from the values determined for the A's and B's in (1): phase is expressed by the local time at which an oscillation maximizes. The horizontal lines in figures 8 to 18 are centred on the least-squares calculated value of a quantity and are equal in length to two standard deviations. At heights where amplitudes are small, phases become indeterminate as indicated by very large error bars or a data point in brackets. Attention has been given to the removal of a background trend in v by replacing v_o in (1) by a polynomial in time. When the total observing time exceeded two days a cubic was adopted. Many series of launchings extend over only one day and in most cases the

analysis of these has been performed with v_o expressed linearly in time: when there were no more than 8 launchings in a series, the background trend was ignored.

9. Diurnal winds at mid-latitudes

The diurnal wind oscillations derived for 23-25 October 1968 and 13-15 December 1967 at Cape Kennedy have previously been compared and discussed (Groves 1976). The results are shown here in figure 8 in comparison with the theoretical phase profiles (the straight lines) for the migrating Hough modes (1,1,1) to (1,1,5): observed phases are seen to correspond most nearly with modes of a higher order than the leading (1,1,1) mode. Phase profiles for 23-25 October 1968 show about 2¼ rotations of the wind vector between 25 and 55 km and are similar to that of the (1,1,3) mode. For 13-15 December 1967 the average gradient of the phase profiles corresponds more closely with that of the (1,1,2) mode.

A notable property of the Cape Kennedy results of 24-26 October 1968 (figure 8) is that the profiles of S-N and W-E amplitudes show no significant differences and that W-E phases at all heights are later than S-N phases by close to 6 hours: in other words, the diurnal wind vector at any given height rotated clockwise with no change of magnitude within the limits of accuracy of the data. If the oscillation may be regarded as a superposition of positive ($n > 0$) Hough modes (1,s,n) then the above property implies approximate equality of W-E and S-N Hough wind functions for each mode that is significantly present. By examination of numerical evaluations of Hough wind functions for various s and n (not demonstrated here) it is found that this apparently stringent condition holds (to within about 20%) at latitudes between 20° and 40° latitude, provided that eastward travelling modes are generally small compared with westward travelling modes.

For the 13-15 December 1967 data, a clockwise rotating wind vector of constant magnitude is found at less than

half the heights analysed, S-N and W-E amplitudes in particular showing significant differences (figure 8). Further analysis of these results in figure 9 shows that whereas the S-N oscillation is steady over the two-day interval that of the W-E component is not: some disturbance would appear to be affecting the W-E tidal oscillation. Although little can be said about the nature of such a disturbance, the direction of slope of the phase profiles (to earlier times with increasing height) points to a source of excitation, that is at lower heights and probably in the troposphere.

Data have now been analysed for diurnal winds at slightly higher latitudes than Cape Kennedy and the results (figures 10 and 11) are found to be generally consistent with the diurnal rotation of a wind vector of approximately constant magnitude at any given height. The number of launchings in each series is shown in Table 1 but data from all launchings may not be available at every height. Reference lines at 12 h and 18 h have been added to the plots of S-N and W-E phases respectively for N hemisphere sites to aid comparisons. The S-N phase profiles at White Sands are quite well reproduced with a 6 h delay by the W-E phase profiles. So also is that for Arenosillo (figure 11). For the S hemisphere site of Mar Chiquita, observed phases are consistent with an anti-clockwise rotation of the wind vector in accord with tidal theory. Mar Chiquita phase profiles have approximately the same average slope as those taken at the same time at Wallops Island which is at the same latitude (within 0.1°) in the opposite hemisphere. A 12 h shift between S-N phases at the two sites therefore indicates a tidal excitation that is predominantly symmetric with respect to the equator; but amplitude profiles differ between the two sites to an extent that suggests that non-migrating modes, i.e. modes that have both local-time and longitudinal dependences, may be significant even for a separation of only 18.1° in longitude.

Results of the White Sands launchings of 30 June-2 July 1965 have previously been reported in some detail by Beyers, Miers & Reed (1966).

10. Diurnal winds at low latitude

S-N and W-E Hough wind functions for positive diurnal modes (not presented here) are found by inspection to become increasingly different in form at latitudes of less than about 15°; and hence at low latitude sites S-N and W-E amplitude and phase profiles would be expected to differ appreciably: the observational results (figures 12 to 15) confirm this expectation.

The results for Antigua show that W-E phases are later than S-N phases by 6 h at most heights except for the interval from 36 to 51 km (figure 12): short wavelengths appear to be propagating in the W-E component below 36 km and in the S-N component below 51 km changing to longer wavelengths above these heights.

Four sets of results for Ascension Island are compared in figure 13. The two sets showing greatest similarity are those for April 1966 which are based on the first 13 and the last 13 launchings of a series of 24 over a 2-day interval. A detailed analysis of the April 1966 data has been given Beyers & Miers (1968) who noted considerable variation in both S-N and W-E components between the two days and concluded that the diurnal variation may have been masked or distorted by some other short-term disturbance. On closely comparing the two sets of April 1966 results in figure 13, it is found that 40 % of the phases on the second day differ significantly from those on the first. The situation is similar to that reported above for 13-15 December 1967 at Cape Kennedy: a steady or quasi-steady tidal oscillation appears to be replaced or dominated by variations which arise from a non-tidal source, i.e. one that does not correlate with the hour angle of the Sun over several days. For other low latitude analyses reported here (figures 14 and 15) it is not possible with the number and distribution of available launchings to compare consecutive cycles, and no indication can therefore be

given of the presence or otherwise of non-tidal effects.

A comparison between the results for Fort Sherman in figure 14 and those taken on the same date (19-20 March 1974) at Ascension Island is of interest as the two sites are at nearly the same latitude in opposite hemispheres. A similar comparison in § 9 for Wallops Island and Mar Chiquita indicated a predominantly symmetric excitation with respect to the equator, but from figures 13 and 14 the Fort Sherman and Ascension Island oscillations are seen to differ markedly in phase and amplitude. These differences may be attributed to the presence of non-tidal effects as discussed above or to the presence of non-migrating modes as referred to in § 9 in conjunction with the 65.6° change of longitude between the two sites. The 19-20 March 1974 results (figure 15) for Kourou and Natal, which are also sites at approximately equal latitudes in opposite hemispheres, again show very dissimilar phase and amplitude profiles.

Also shown in figure 15 are results obtained by the acoustic--grenade technique at Natal (Groves 1974) and Kourou (Groves 1975a). The Natal launchings differ from the other launch series on account of their distribution over an interval of 22 months consequently the results from them would be expected to reveal a component of oscillation that is steady for much of the year. The Kourou acoustic-grenade phase profiles (figure 15) match those for Natal of 1966-68 to a remarkable extent except at the lower heights. As reported previously however (Groves 1975a) the Kourou tempterature oscillation showed significant differences from that for Natal indicating some variation in the source of excitation for which the atmospheric response was of observational significance in temperature and not in winds. Further evidence of variation in the source of excitation between different dates is provided by the 19-20 March 1974 wind results

at Natal and Kourou which differ significantly from the acoustic-grenade results at the corresponding sites (figure 15).

11. Diurnal winds at Fort Churchill

It is a well-known property of diurnal Hough functions (Chapman & Lindzen 1970, Groves 1975b) that positive modes are confined to low and mid latitudes, whereas negative modes attain their greatest values at high latitudes. At Fort Churchill tidal oscillations can therefore be expected to be composed of negative modes. Another property of negative modes is that in contrast to the vertically propagating and oscillatory nature of positive modes they show no rotation in height and have amplitudes that decay in either vertical direction away from the level of excitation, such that stratospheric oscillations would be excited by stratospheric (ozone) heating. The height independence of phase at high latitude was confirmed by the analysis of Reed et al. (1969) of summer data between 30 and 60 km from the combined stations of Fort Churchill and Fort Greely for the diurnal S-N wind oscillation: observed S-N wind phases were very close to 12 noon, the value which accords theoretically with an expected 12 noon phase for the ozone heating rate.

Figure 16 shows S-N and W-E diurnal winds for Fort Churchill obtained from series of launchings conducted on the dates shown. The results are independent of those of Reed et al. (1969) which were derived from data widely distributed in time over the summer months of several years prior to and including 1966. S-N phases at or close to 12 noon are common in figure 16 with the notable exceptions, to be discussed in the next paragraph, of 4-5 January 1968 and certain heights below 45 km. For the W-E wind oscillation the corresponding theoretical phase is 1800 h the rotation of the wind vector being clockwise. With

the same exceptions this value is fairly well supported observationally. The two launch series in September 1966 comprise the first 10 and the last 10 launchings respectively of a series of 19 launchings at 4 h intervals over 3 days. The general form of the phase profiles in figure 16 clearly differs in character from that at other latitudes (figures 8 to 15) where positive modes are able to propagate.

Below 40 km ozone lifetimes increase sufficiently for atmospheric motion to become an effective transport mechanism and longitudinal asymmetries in ozone distribution arise (Heath et al. 1973; Krueger et al. 1973; Dütsch 1974). Maximum heating rates may then be displaced in longitude from the subsolar longitude and phases of the S-N wind below about 45 km would not necessarily be at 12 noon. In the absence of information on ozone distributions such relationships cannot however be examined . The unusual phase profiles of 4-5 January 1968 also direct attention to the possibility of a disturbed ozone distribution, in this case up to 55 km, and considering the time of year this might arise from a stratospheric warming and its effect on temperature-dependent photochemistry (Barnett et al. 1975). On examining M.N.R. synoptic charts of N. America, it is found that this series of launchings coincided with a major warming which started in December 1967 and persisted into the beginning of 1968: by the end of December, the temperature gradient between polar and mid latitudes had reversed throughout the entire middle and upper stratosphere making the event the earliest major warming ever to be recorded (ESSA 1970; NOAA 1971). Of the other above Fort Churchill launchings none took place at the time of a stratospheric warming.

12. Semidiurnal winds at latitudes greater than 30°

Figure 17 shows semidiurnal wind phases and amplitudes at six different sites, data being available at Fort

Churchill for four different dates. The 19 launchings of 6-9 September 1960 at Fort Churchill have been divided into two groups consisting of the first 10 and the last 10 launchings respectively: each group extends over three consecutive cycles and the results of the first group are quite well reproduced by the second group indicating the presence of quite a speady oscillation over this 3-day interval. Comparisons between other sets of results are, in contrast, notable for conspicuous differences in phase and amplitude profiles.

One feature which stands out in Figure 17 is that S-N and W-E profiles show similarities of phase and to a lesser extent of amplitude, W-E phases being later than S-N phases by close to 3 h corresponding to a clockwise rotation of the wind vector. For the S hemisphere site of Mar Chiquita an anticlockwise rotation is indicated.

Another feature of the phase profiles in figure 17 is their failure to comply with previous theoretical results for semidiurnal oscillations which present a mainly constant phase arising from the assumed predominance of the (2,2,2) mode. In the classical treatment (Chapman & Lindzen 1970) a rapid phase reversal is obtained just below 30 km between adjacent regions of almost constant phase extending up to the mesopause and down to the surface. In the more recent calculations of Lindzen & Hong (1974) with a more realistic atmosphere, the chief modification is to the level at which the reversal occurs.

Interpretation of the results in figure 17 in terms of tidal Hough modes requires the introduction of significant contributions from higher-order semidiurnal modes. Some guide to the order of modes present is provided by the phase profiles which for particular height ranges complete one rotation (i.e. 12 h change of phase) within 14 km or less of vertical distance. Among the migrating

semidiurnal modes those having such oscillatory structures would be (2,2,n) where $n \geq 14$. As with the diurnal components (§ 9) the direction of slope of the phase profiles (to earlier times with increasing height) points to a source of excitation at lower heights, most probably in the troposphere, where a common identity would be expected with the source of excitation of the diurnal components.

The above account of the properties of the semidiurnal oscillations closely follows that previously given (Groves 1976) on the basis of the Fort Churchill results of 6-9 September 1966 and 23-25 October 1968 and the Wallops Island and Mar Chiquita results of 19-20 March 1974. The further observations that have since been analysed and now appear in figure 17 support the previous account. The similarity between S-N and W-E semidiurnal profiles at mid and high latitudes and the clockwise rotation of the wind vector at N latitudes and anticlockwise rotation at S latitudes are in accord with the properties of Hough wind functions as previously discussed (Groves 1976). These properties were previously examined for migrating modes (2,2,n) and further calculations (not presented here) show that they also hold for both eastward and westward travelling non-migrating modes (2,s,n), $s \neq 2$.

13. Semidiurnal winds at latitudes less than 30°

Figure 18 shows sets of results of semidiurnal oscillations derived at sites of less than 30° latitude. The two sets of results for Cape Kennedy at 28.5°N are consistent with a clockwise rotating wind vector at most observation heights within the limits of error and could be grouped with the results in figure 17. For Antigua at 17°N and also at still lower latitudes S-N and W-E

Hough wind functions become appreciably dissimilar and corresponding dissimilarities are to be expected between S-N and W-E semidiurnal wind components. The observational results for Antigua, Fort Sherman and most other launch sites in figure 18 show conspicuous differences between S-N and W-E components which would appear to confirm this expectation.

The analyses for Ascension Island on 11-12 and 12-13 April 1966 (figure 18) show that both S-N and W-E semidiurnal components change radically between the two days. As with the diurnal components at low latitude (§10), a non-tidal variation would appear at times to replace or dominate a steady or quasi-steady tidal oscillation. Insufficient data are available to examine the frequency of such occurrences.

14. Discussion

14.1 Seasonal wind variations

Meridional cross-sections of S-N and W-E wind components from 60 to 130 km at monthly intervals were prepared in 1969 and similar W-E wind models appear in CIRA 1972. These cross-sections were prepared by averaging and smoothing observed wind components and have provided reference models against which to compared newly acquired data. Recent wind measurements by radio tecnniques, 80 to 100 km, tend to confirm the main features of the models and their seasonal trends. Although many of the recent observations are from new longitudes, data coverage is still inadequate to allow reliable zonal mean motions to be obtained. With the new data however zonal means would now appear unlikely to differ greatly from model values and in particular from the high ($\sim$10 m/s) S-N model velocities at heights close to 90 km.

Consideration has been given in § 5 to the mean meridional circulation that may be inferred from the wind models by reference to the 1974 calculations of Ebel for vertical wind velocities and by interpretation of the sloping zero S-N velocity line in the winter hemisphere of figure 1 as a boundary region separating mesospheric and lower thermospheric circulation patterns. The wintertime circulation described is an average situation appropriate to a time interval of the order of a month from which appreciable deviations are indicated on shorter time-scales by, for example, the day-to-day wind variations that are observed close to 90 km. Long-term variations, such as a solar cycle dependence for winter-time winds, have been identified in mean meridional winds at particular sites and indicate corresponding long-term modulations of the circulation.

Meridional circulations in the middle atmosphere cannot be studied observationally without an extensive coverage of global wind data that is far in excess of that available or likely to be available for some time. Evidence of the nature of meridional transport may however be indirectly obtained if other observable effects exist that are dependent upon it. Two ways in which wintertime mean meridional circulations may be relevant to middle atmosphere aeronomy are considered to be worthy of further examination: these are the mixing of air of mesospheric-equatorial origin with that of thermospheric-polar origin at about 90 km over mid-latitudes and the effect of such circulations on the internal atmospheric conditions appropriate to the winter anomaly in radio-wave absorption.

14.2 Diurnal variations

The principal frequency components of wind variations at meteor ionization heights are solar diurnal and semidiurnal (Teptin 1972): the same components predominate in surface pressure oscillations (Chapman & Lindzen 1970). In §§ 7 to 13 diurnal and semidiurnal components obtained from short series of rocket launchings are presented and discussed for the intermediate region of approximately 25 to 60km.

The results of early series of launchings at White Sands and Ascension Island for diurnal components have previously been reported (Beyers, Miers & Reed 1966; Beyers & Miers 1968): the conclusion reached was that a dominant diurnal tidal oscillation existed at the stratopause at the mid-latitude site whereas at the low-latitude site a well-defined diurnal variation was not evident being masked or distorted by some other short-term disturbance. The larger body of data that has now been analysed supports these conclusions with the rider that at low latitudes both diurnal and semidiurnal variations are affected by short-term disturbances although only intermittently. Greater clarification of the frequency of such disturbances cannot be given with the very few sets of data available.

Comparisons between phase and amplitude profiles for the same location at different times rarely show similarities and it would seem that at these heights the tidal motions are steady for only short intervals of time, possibly a few days, although no reliable estimate can be given of this variability as data are not available over adequate intervals of time.

It has also been possible to compare results at different stations at the same time including pairs of stations at almost the same latitude in opposite hemispheres (Wallops Island/Mar Chiquita, Kourou/Natal

and Fort Sherman/Ascension Island). Comparisons between phase and amplitude profiles rarely show similarities indicating a detailed horizontal structure to tidal motions including a longitudinal dependence. From the longitudinal separation of the above pairs of stations, variations are significant over distances of $\sim 10^3$ km.

At latitudes greater than about 30° phase profiles of W-E and S-N wind components usually represent wind vectors that rotate with height (clockwise in the N hemisphere and anti-clockwise in the S hemisphere). Rates of rotation with height are however greater than those corresponding to excitation of the leading diurnal or semidiurnal modes being appropriate to higher-order modes whose latitudinal structure would require significant variations in the source of excitation over $\sim 10^\circ$ changes of latitude. Support for the interpretation of observed oscillations in terms of tidal modes is provided by phase profiles at high latitude (Fort Churchill) which differ characteristically from those at lower latitudes for the diurnal component but not for the semidiurnal: the diurnal phases at Fort Churchill are more nearly constant with respect to height than those at lower latitudes in accord with the properties of positive and negative sequences of diurnal modes, whereas for the semidiurnal component only one sequence of modes exists.

An area for further investigation is the identification of the relatively localized sources of excitation that seem to be implied by the observations. Significant variations in tropospheric conditions over distances of $\sim 10^3$ km are common enough, but the requirement is for steady or quasi-steady diurnal and semidiurnal frequency components of an adequate magnitude to generate the stratospheric winds observed.

Acknowledgements

The author gratefully acknowledges the assistance of Miss A.M. Yeung with analysis of data and of Miss U. Campbell and members of the Departmental Photographic Group with preparation of diagrams. Sponsorship has been provided by the Air Force Geophysics Laboratory (AFGL), United States Air Force under Grant No. AFOSR--77-3224 and by the U.K. Meteorological Office.

References

Belmont, A.D., Nastrom, G.D. & Hovland, D.N. 1977 Periodic Wind Variations at 65-118 km at Saskatoon (52°N), Control Data Corporation Final Report dated 26 May 1977, Minneapolis, Mn., USA.

Beyers, N.J. and Miers, B.T. 1968 J. atmos. Sci. 25, 155-159.

Beyers, N.J., Miers, B.T. & Reed, R.J. 1966 J. atmos Sci. 23, 325-333.

Chapman, S. & Lindzen, R.S. 1970 Atmospheric tides: thermal and gravitational, Dordrecht, Holland: D. Reidel Publisning Co.

CIRA 1972 COSPAR International Reference Atmosphere, Akademie-Verlag, Berlin.

Clark, R.R. 1975 J. atmos. Sci. 32, 1689-1693.

Dütsch, H.U. 1974 Can. J. Chem. 52, 1491-1504.

Ebel, A. 1974 Tellus 26, 325-333.

Elford, W.G. 1976 Nature(Lond.) 261, 123-124.

ESSA 1970 Weekly Synoptic Analyses, 5-, 2-, and 0.4-Millibar Surfaces for 1967, ESSA Technical Report WB 12.

Glass, M., Fellous, J.L., Massebeuf, M., Spizzichino, A., Lysenko, I.A. & Portniaghin, Yu. I. 1975 J. atmos. terr. Phys. 37, 1077-1087.

Gregory, J.B. & Manson, A.H. 1975 J. atmos. Sci. 32, 1667-1675.

Gregory, J.B. & Rees, D.T. 1971 J. atmos Sci. 28, 1079-1082.

Groves, G.V. 1967 Space Research 7, 986-1000.

Groves, G.V. 1969 J. Br. interplanet. Soc. 22, 285-307.

Groves, G.V. 1974 J. Br. interplanet. Soc. 27, 499-511.

Groves, G.V. 1975a J. Br. interplanet. Soc. 28, 241-244.

Groves, G.V. 1975b J. Br. Interplanet. Soc. 28, 797-809.

Groves, G.V. 1976 Proc. R. Soc. Lond. A 351, 437-469.

Heath, D.F., Mateer, C.L. & Krueger, A.J. 1973 Pure appl. Geophys. 106-108, 1238-1253.

Kellogg, W.W. 1961 J. Meteor. 15, 373-381.

Kreuger, A.J., Heath, D.F. & Mateer, C.L. 1973 Pure appl. Geophys. 106-108, 1253-1263.

Laštovička, J. 1972 J. atmos. terr. Phys. 34, 1233-1239.

Leovy, C. 1964 J. atmos. Sci. 21, 327-341.

Lindzen, R.S. & Hong, S.S. 1974 J. atmos. Sci. 31, 1421-1446.

Lysenko, I.A., Portnyagin, Yu. I., Greisiger, K.M. & Sprenger, K. 1975 Zeit. f. Meteorologie 25, 213-217.

Muller, H.G. and Kingsley, S.P. J. atmos. terr. Phys. 36, 1933-1943.

NOAA 1971 Weekly Synoptic Analyses, 5-, 2-, and 0.4 -Millibar Surfaces for 1968, NOAA Technical Report NWS 14.

Portnjagin, Ju. I., Kaidalov, O.V., Greisiger, K.M. & Sprenger, K. 1977 Phys. Solariterr. Potsdam, No. 5, 91-96.

Reed, R.J., Oard, M.J. & Sieminski, M. 1969 Mon. weath. Rev. 97, 456-469.

Roper, R.G. 1975 Radio Sci. (USA) 10, 363-369.

Rose, G., Widdel, H.U., Azcárraga, A. & Sanchez, L. 1972a Phil. Trans. R. Soc. Lond A271, 529-545.

Rose, G., Widdel, H.U., Azcárraga, A. & Sanchez, L. 1972b Phil. Trans. R. Soc. Lond. A 271, 509-528.

Schmidlin, F.J., Yamasaki, Y., Motta, A. & Brynsztein, S. 1975 N.A.S.A. sp-3095, Washington, D.C.

Scholefield, A.J. & Alleyne, H. 1975 J. atmos. terr. Phys. 37, 273-286.

Smith, W.S., Theon, J.S., Casey, J.F. & Horvath, J.J. 1970 N.A.S.A. TR R-340, Washington, D.C.

Smith, W.S., Theon, J.S., Swartz, P.C., Casey, J.F. & Horvath, J.J. 1969 N.A.S.A. TR R-316, Washington, D.C.

Smith, W.S., Theon, J.S., Swartz, P.C., Katchen, L.B. & Horvath, J.J. 1968 N.A.S.A. TR R-288, Washington, D.C.

Smith, W.S., Theon, J.S., Wright, Jr., D.U., Ramsdale, D.J. & Horvath, J.J. 1974 N.A.S.A. TR R-416, Washington, D.C.

Sprenger, K., Greisiger, K.M. & Schminder, R. 1975 J. atmos. terr. Phys. 37, 1391-1393.

Sprenger, K. & Schminder, R. 1969 J. atmos. terr. Phys. 31, 217-221.

Stubbs, T. J. 1976 J. atmos. terr. Phys. 38, 979-989.

Teptin G.M. 1972 Acad. Sci.USSR, Atmosph.& Oceanic. Phys. 8, 139-150.

Vincent, R.A. & Stubbs, T.J. 1977 Planet. Space Sci. 25, 441-455.

Wilkinson, P.J. & Baggaley, W.J. 1975 Planet. Space Sci. 23, 509-522.

TABLE 1. Diurnal launch series 1965-74.

Site	lat.	long.W	date	no. of successful launchings
Thule	76°33'N	68°49'	24-26 Oct 1968	14
Fort Churchill	58°44'	93°49'	6-8 Sept 1966	10
			8-9 Sept 1966	10
			4-5 Jan 1968	12
			23-25 Oct 1968	18
			19-20 Mar 1974	8
Wallops Is.	37°50'	75°29'	19-20 Mar 1974	13
Arenosillo	37°06'	06°44'	24-28 Feb 1970	27
White Sands	32°23'	106°29'	30 Jun-2 Jul 1965	17
			9-11 Oct 1965	16
Cape Kennedy	28°27'	80°32'	13-15 Dec 1967	25*
			23-25 Oct 1968	17
Antigua	17°09'	61°47'	19-20 Mar 1974	8
Fort Sherman	09°20'	79°59'	19-20 Mar 1974	8
Kourou	05°08'	52°37'	19-22 Sept 1971	13
			19-20 Mar 1974	10
Natal	05°55'S	35°10'	1966-68	24
			19-20 Mar 1974	8
Ascension Is.	07°59'	14°25'	11-12 Apr 1966	13
			12-13 Apr 1966	13
			24-26 Oct 1968	14
			19-20 Mar 1974	8
Mar Chiquita	37°45'	57°25'	19-20 Mar 1974	7

* Also analysed as 13-14 Dec 1967 (12 launchings) and 14-15 Dec 1967 (14 launchings).

LEGENDS

FIGURE 1. Meridional cross-sections of W-E winds (above) and S-N winds (below) in m/s for 1 January. E denotes winds from the east (Groves 1969).

FIGURE 2. The 24 h averages of S-N wind components taken at weekly intervals by the Jamaica meteor-radar technique. The dashed curve is the 1969 S-N wind model for 15°N (Scholefield and Alleyne 1975).

FIGURE 3. S-N prevailing wind components at Adelaide, S. Australia. Key: —— observed ionospheric drift by partial reflection technique 15-21 June 1973; - - - - the 1969 S-N wind model for the same latitude and time of year (Vincent & Stubbs 1977).

FIGURE 4. S-N prevailing wind components for winter 1972-73 at 95 km. Key: —— Obninsk; ..... Kühlungsborn/Collm (Lysenko et al. 1975).

FIGURE 5. Prevailing S-N wind components at 95 km for the winter months November-February plotted against solar 10.7 cm radio flux. Data are from Kühlungsborn/Collm (1957/58-1974/75) and Obninsk (1964/65-1972/73) (Portnjagin et al. 1977).

FIGURE 6. Variation with latitude of the mean velocity component normal to the isobaric surfaces at heights of about 72, 85 and 95 km in the N hemisphere for January 1 and July 1. Positive values represent upward motion (Ebel 1974).

FIGURE 7. The eight sites from which diurnal series of rockets were launched on 19-20 March 1974.

FIGURE 8. Diurnal wind components at Cape Kennedy. The straight lines indicate the approximate theoretical slopes of the phase profiles of the first five positive migrating modes.

FIGURE 9. Diurnal wind components on two consecutive days at Cape Kennedy. (1) 13-14 December 1967; (2) 14-15 December 1967.

FIGURE 10. Diurnal wind components at White Sands, Wallops Island and Mar Chiquita.

FIGURE 11. Diurnal wind components at Arenosillo, 24-28 February 1970.

FIGURE 12. Diurnal wind components at Antigua, 19-20 March 1974.

FIGURE 13. Diurnal wind components at Ascension Island. (1) 11-12 April 1966; (2) 12-13 April 1966; (3) 24-26 October 1968; (4) 19-20 March 1974.

FIGURE 14. Diurnal wind components at Fort Sherman, 19-20 March 1974.

FIGURE 15. Diurnal wind components at Kourou and Natal. (1) Kourou, 19-22 September 1971; (2) Kourou, 19-20 March 1974; (3) Natal, 1966-68; (4) Natal, 19-20 March 1974.

FIGURE 16. Diurnal wind components at Fort Churchill.

FIGURE 17. Semidiurnal wind components at latitudes greater than 30°. (1) Thule, 24-26 October 1968; (2) Fort Churchill, 6-8 September 1966; (3) Fort Churchill, 8-9 September 1966; (4) Fort Churchill, 4-5 January 1969; (5) Fort Churchill, 23-26 October 1968; (6) Fort Churchill, 19-20 March 1974; (7) Wallops Island, 19-20 March 1974; (8) Mar Chiquita, 19-20 March 1974; (9) Arenosillo, 24-28 February 1970; (10) White Sands, 30 June-2 July 1965; (11) White Sands, 9-11 October 1965.

FIGURE 18. Semidiurnal wind components at latitudes less than 30°. (1) Cape Kennedy, 13-15 December 1967; (2) Cape Kennedy, 23-25 October 1968; (3) Antigua, 19-20 March 1974; (4) Fort Sherman, 19-20 March 1974; (5) Kourou, 19-22 September 1971; (6) Kourou, 19-20 March 1974; (7) Natal, 19-20 March 1974; (8) Ascension Island, 11-12 April 1966; (9) Ascension Island, 12-13 April 1966; (10) Ascension Island, 24-26 October 1968; (11) Ascension Island, 19-20 March 1974.

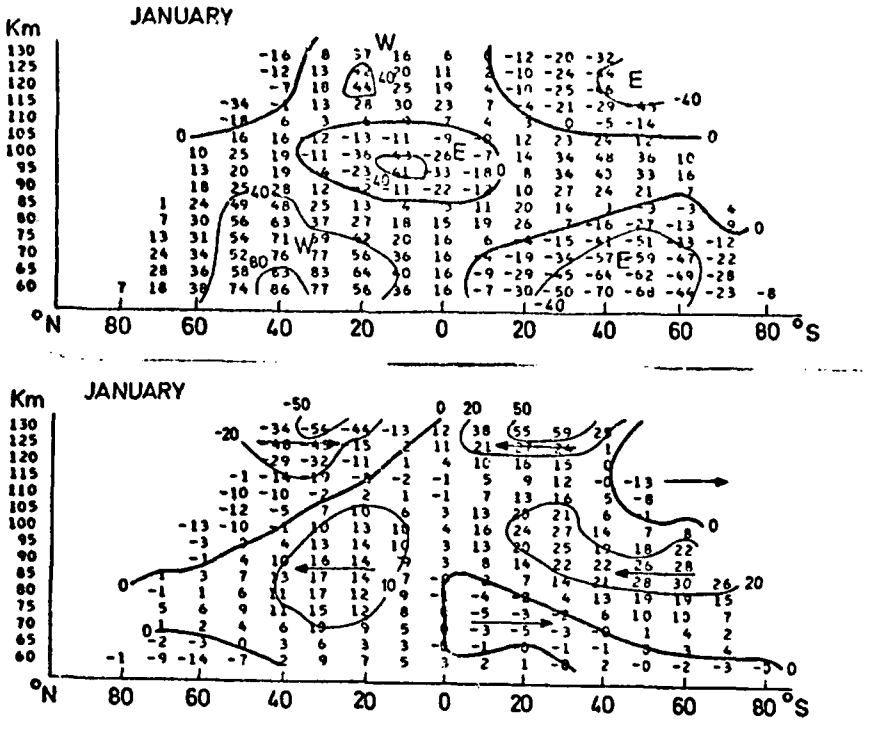

FIGURE 1. Meridional cross-sections of W-E winds (above) and S-N winds (below) in m/s for 1 January. E denotes winds from the east (Groves 1969).

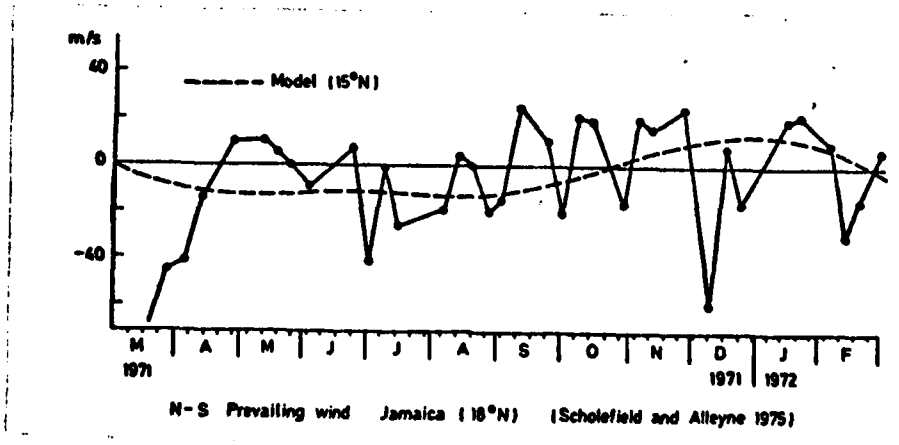

FIGURE 2. The 24 h averages of S-N wind components taken at weekly intervals by the Jamaica meteor-radar technique. The dashed curve is the 1969 S-N wind model for 15° (Scholefield and Alleyne 1975).

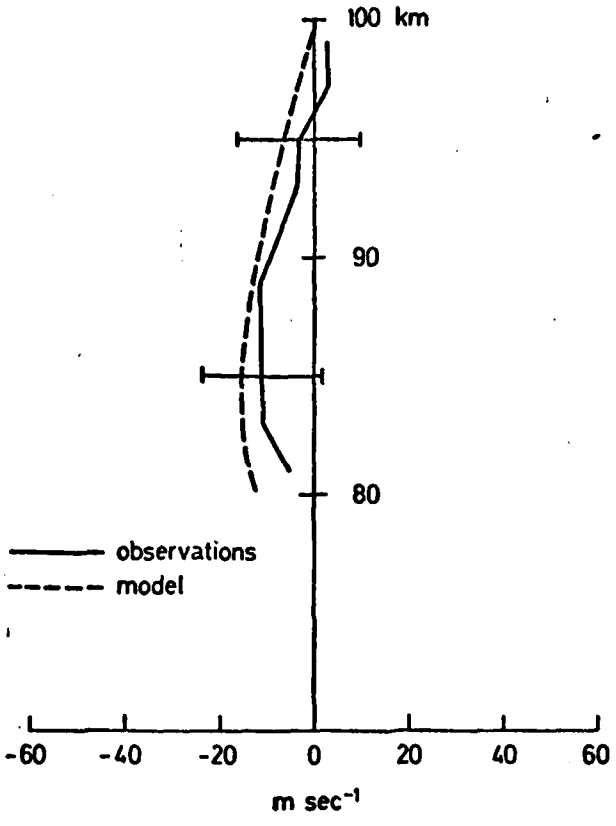

FIGURE 3. S-N prevailing wind components at Adelaide, S. Australia. Key: —— observed ionospheric drift by partial reflection technique 15-21 June 1973; - - - - the 1969 S-N wind model for the same latitude and time year (Vincent & Stubbs 1977).

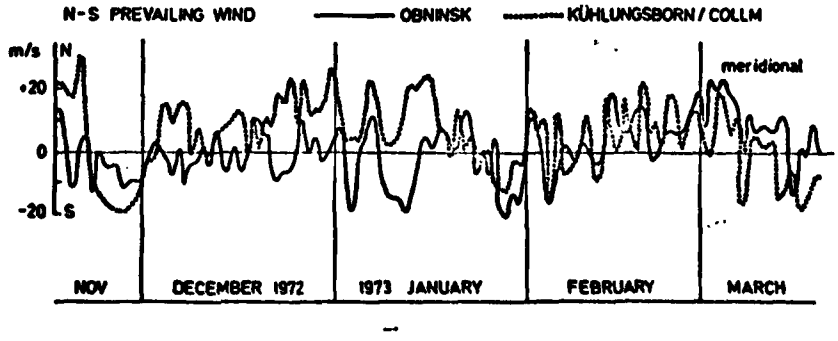

FIGURE 4. S-N prevailing wind components for winter 1972-73 at 95 km. Key —— Obninsk; ..... Kühlungsborn/Collm (Lysenko et al. 1975).

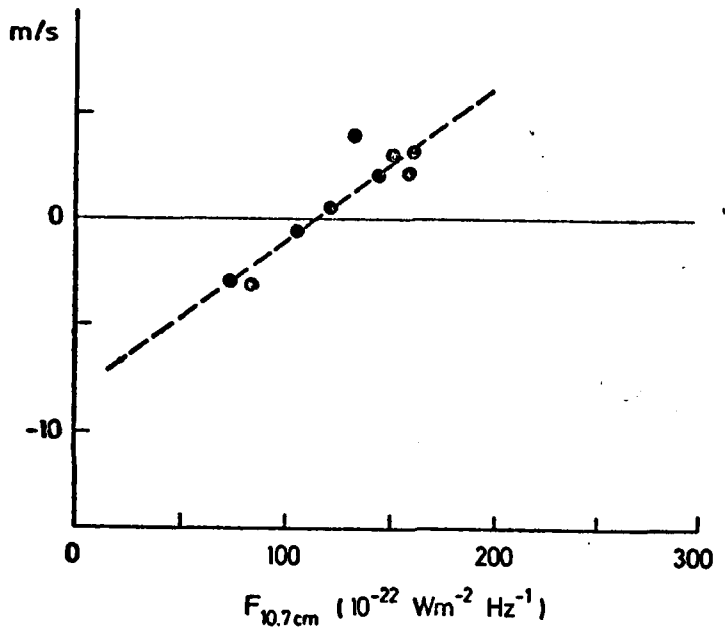

FIGURE 5. Prevailing S-N wind components at 95 km for the winter months November-February plotted against solar 10.7 cm radio flux. Data are from Kühlungsborn/Collm (1957/58-1974/75) and Obninsk (1964/65-1972/73) (Portnjagin et al. 1977).

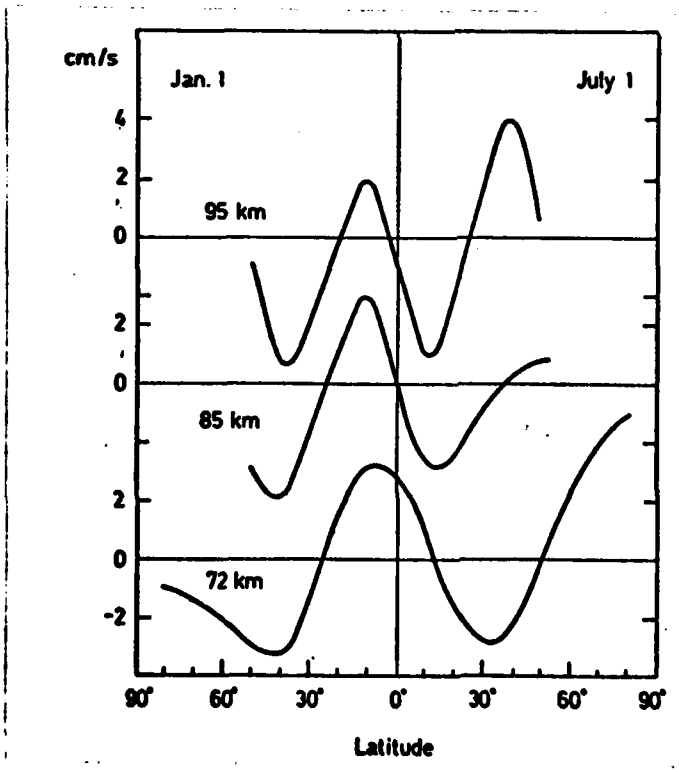

FIGURE 6. Variation with latitude of the mean velocity component normal to the isobaric surfaces at heights of about 72, 85 and 95 km in the N hemisphere for January 1 and July 1. Positive values represent upward motion (Ebel 1974).

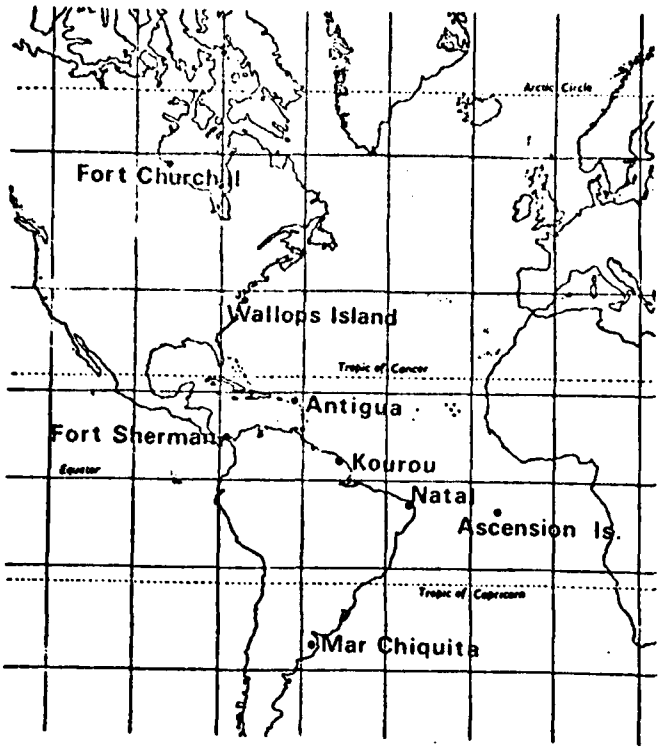

The eight sites from which the diurnal series of rockets were launched on 19 - 20 March 1974.

FIGURE 7.

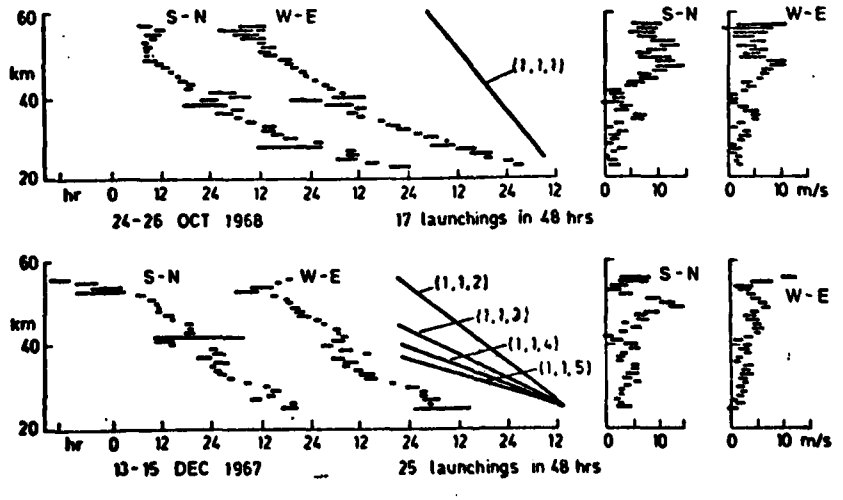

FIGURE 8. Diurnal wind components at Cape Kennedy. The straight lines indicate the approximate theoretical slopes of the phase profiles of the first five positive migrating modes.

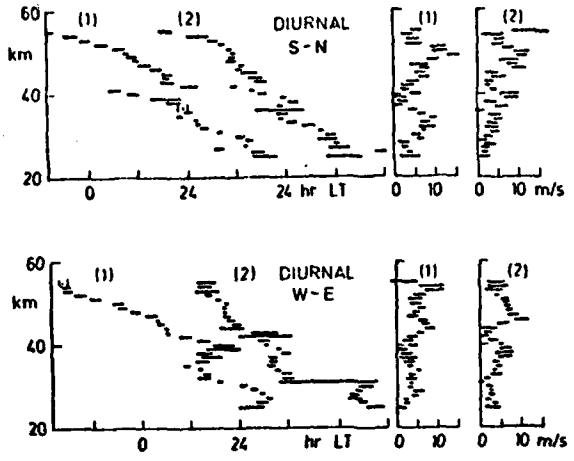

FIGURE 9. Diurnal wind components on two consecutive days at Cape Kennedy. (1) 13-14 December 1967; (2) 14-15 December 1967.

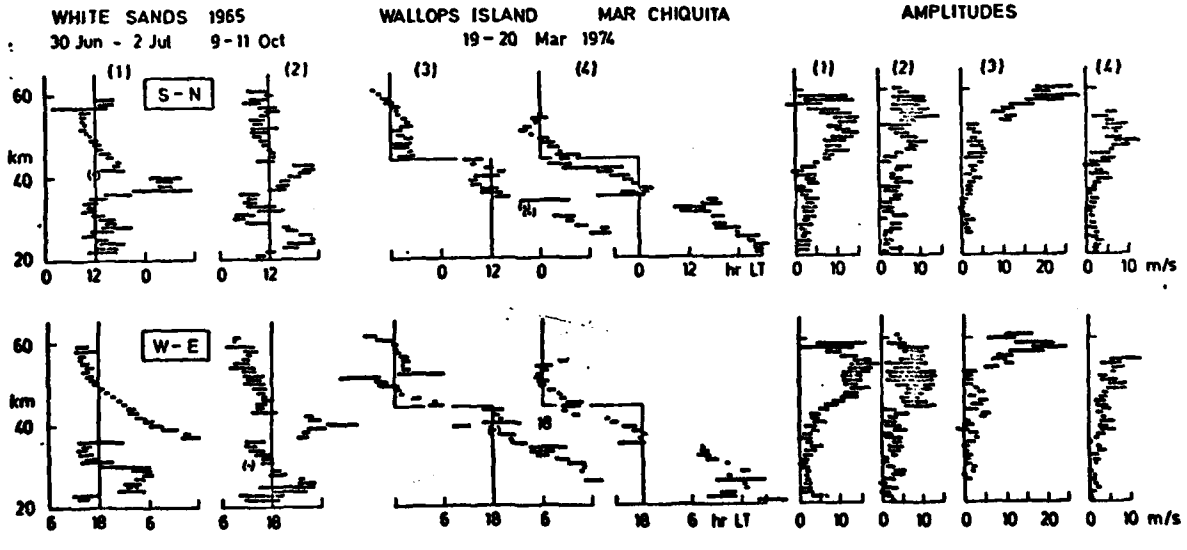

FIGURE 10. Diurnal wind components at White Sands, Wallops Island and Mar Chiquita.

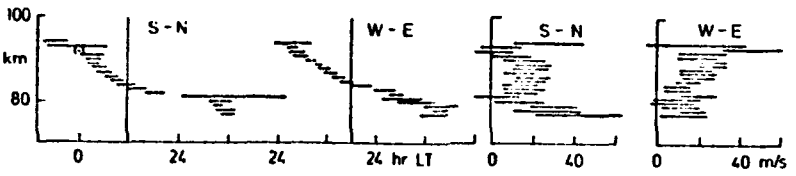

FIGURE 11. Diurnal wind components at Arenosillo, 24-28 February 1970.

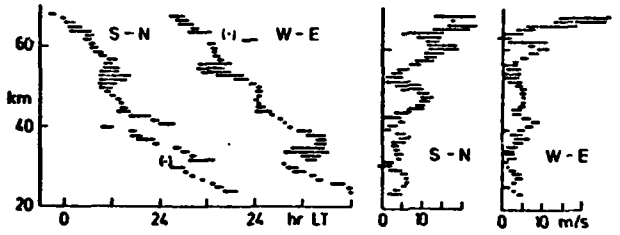

FIGURE 12. Diurnal wind components at Antigua, 19-20 March 1974.

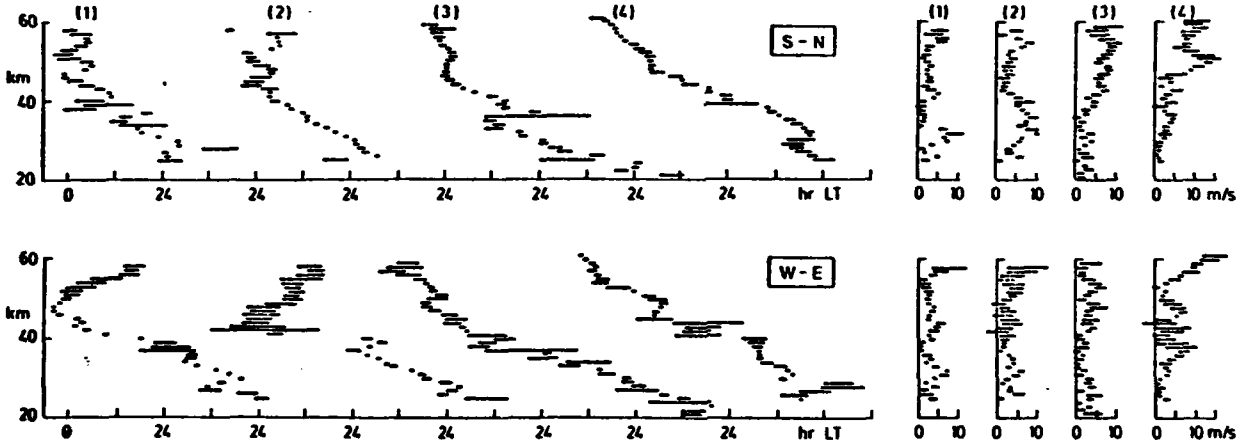

FIGURE 13. Diurnal wind components at Ascension Island. (1) 11-12 April 1966; (2) 12-13 April 1966; (3) 24-26 October 1968; (4) 19-20 March 1974.

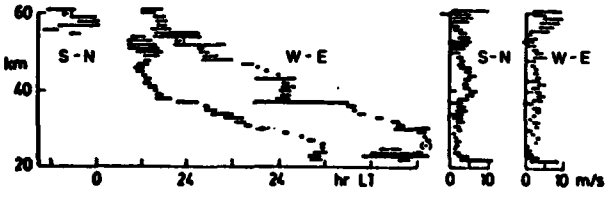

FIGURE 14. Diurnal wind components at Fort Sherman, 19-20 March 1974.

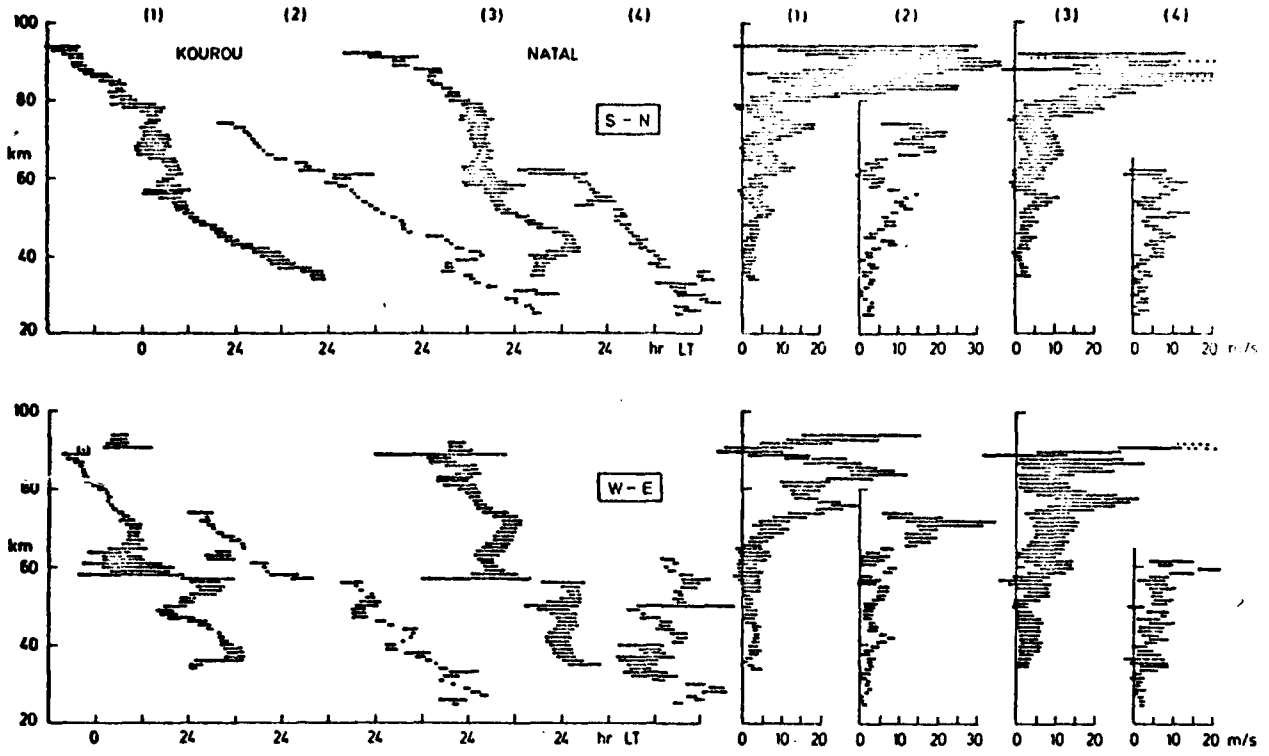

FIGURE 15. Diurnal wind components at Kourou and Natal. (1) Kourou, 19-22 September 1971; (2) Kourou, 19-20 March 1974; (3) Natal, 1966-68; (4) Natal, 19-20 March 1974.

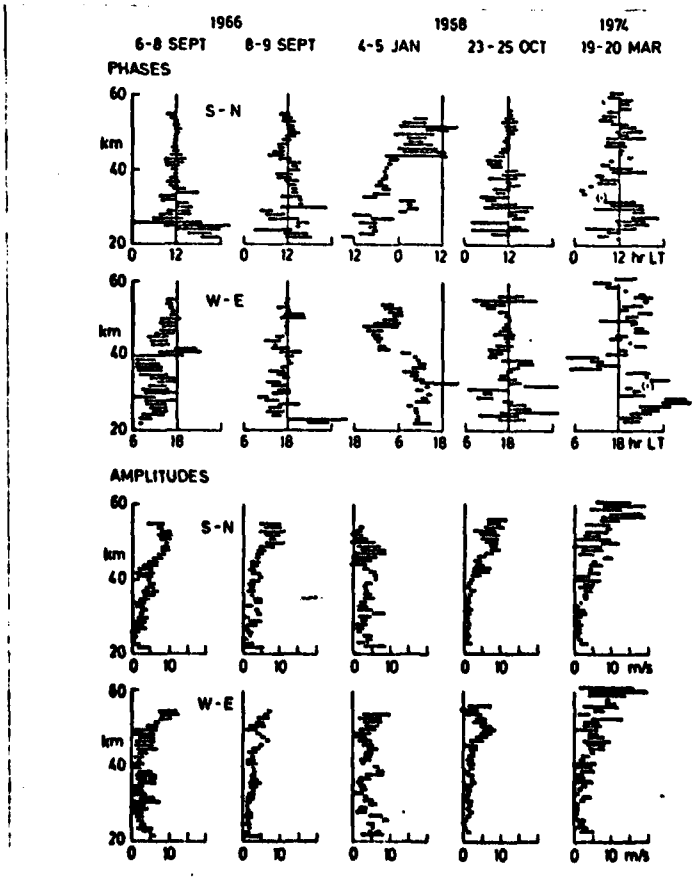

FIGURE 16. Diurnal wind components at Fort Churchill.

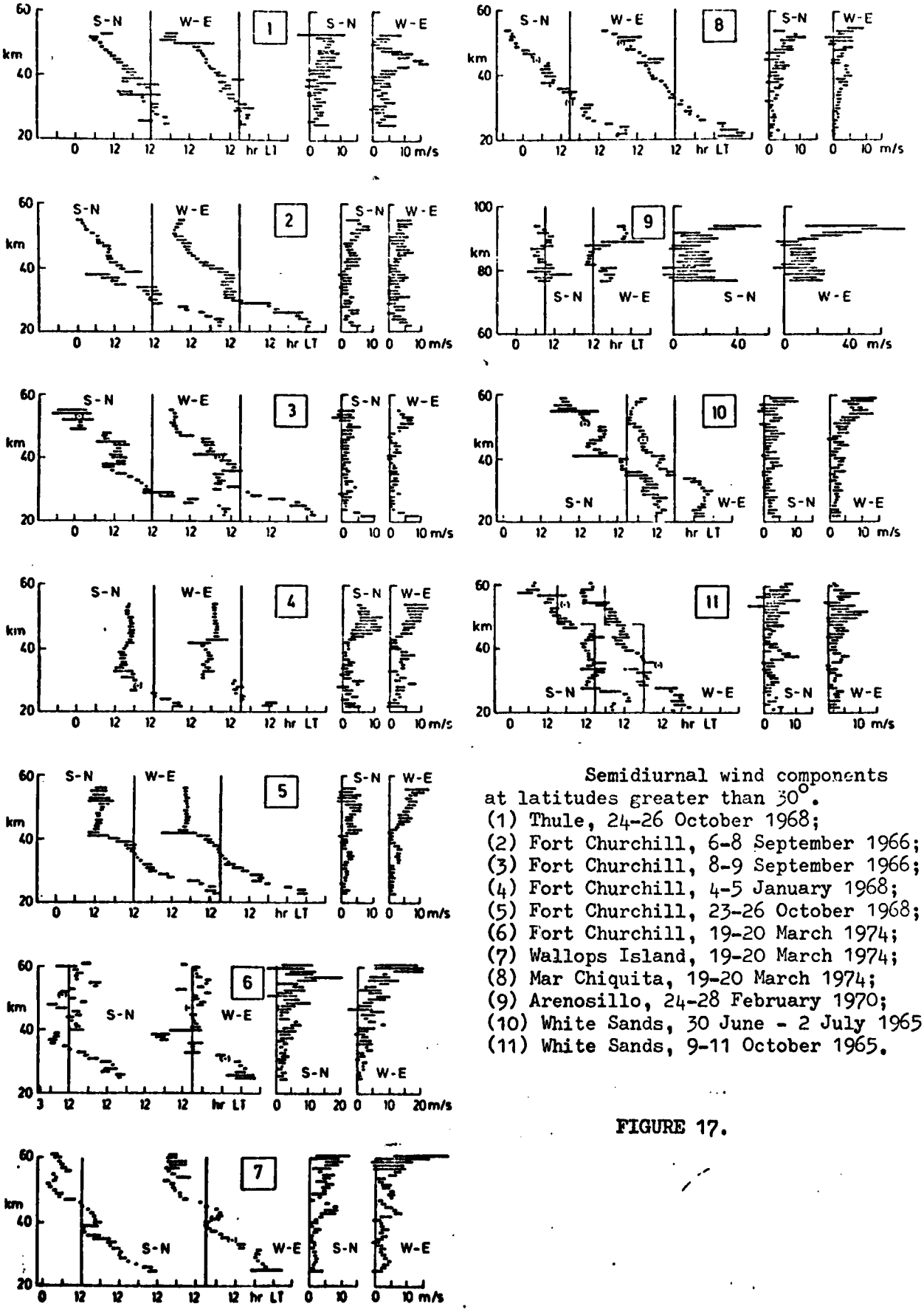

Semidiurnal wind components at latitudes greater than 30°.
(1) Thule, 24-26 October 1968;
(2) Fort Churchill, 6-8 September 1966;
(3) Fort Churchill, 8-9 September 1966;
(4) Fort Churchill, 4-5 January 1968;
(5) Fort Churchill, 23-26 October 1968;
(6) Fort Churchill, 19-20 March 1974;
(7) Wallops Island, 19-20 March 1974;
(8) Mar Chiquita, 19-20 March 1974;
(9) Arenosillo, 24-28 February 1970;
(10) White Sands, 30 June - 2 July 1965;
(11) White Sands, 9-11 October 1965.

FIGURE 17.

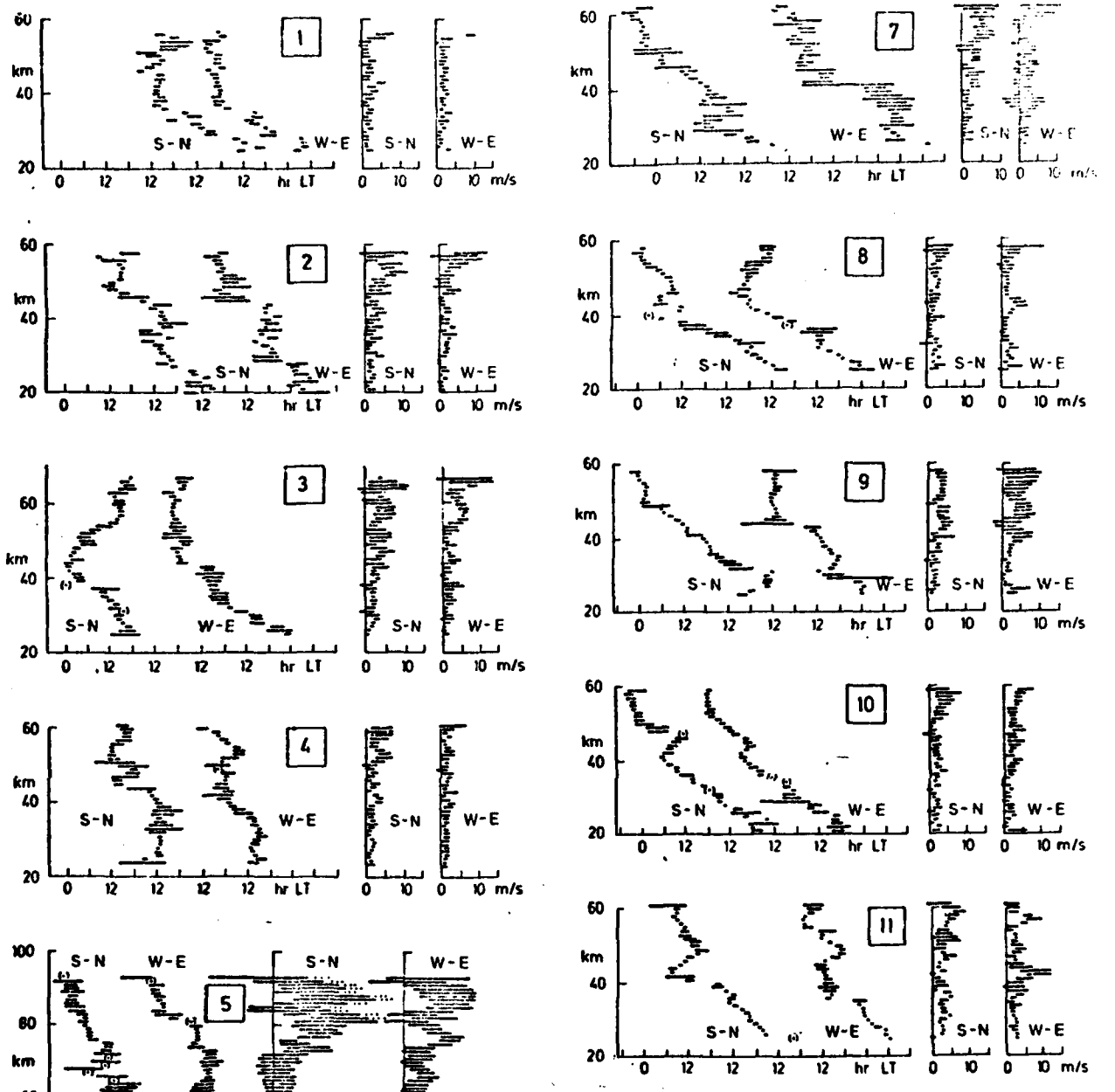

Semidiurnal wind components at latitudes less than 30°.
(1) Cape Kennedy, 13-15 December 1967;
(2) Cape Kennedy, 23-25 October 1968;
(3) Antigua, 19-20 March 1974;
(4) Fort Sherman, 19-20 March 1974;
(5) Kourou, 19-22 September 1971;
(6) Kourou, 19-20 March 1974;
(7) Natal, 19-20 March 1974;
(8) Ascension Island, 11-12 April 1966;
(9) Ascension Island, 12-13 April 1966;
(10) Ascension Island, 24-26 October 1968;
(11) Ascension Island, 19-20 March 1974.

FIGURE 18.